INTERNATIONAL ATOMIC ENERGY AGENCY
UNITED NATIONS EDUCATIONAL, SCIENTIFIC AND CULTURAL ORGANIZATION
INTERNATIONAL CENTRE FOR THEORETICAL PHYSICS
I.C.T.P., P.O. BOX 586, 34100 TRIESTE, ITALY. CABLE CENTRATOM TRIESTE

H4.SMR/449-18

WINTER COLLEGE ON
HIGH RESOLUTION SPECTROSCOPY

(8 January - 2 February 1990)

POPULATION TRANSFER BETWEEN MOLECULAR VIBRATIONAL LEVELS I: A NEW CONCEPT (STIRAP) AND EXPERIMENTAL RESULTS

K. Bergmann
U. Gaubatz*, P. Rudecki**
S. Schiemann

Universität Kaiserslautern
Fachbereich Physik
Kaiserslautern D6750
F.R. Germany

(*) State University of New York
Dept. of Physics
Stony Brook, New York 11794-800, U.S.A.

(**) Nicolaus Copernicus University
Dept. of Physics
87 - 100 Torun
Poland

Population transfer between molecular vibrational levels I : A new concept (STIRAP) and experimental results

U.Gaubatz*, P.Rudecki**, S.Schiemann, and K.Bergmann

Fachbereich Physik der Universität, Postfach 3049,
6750 Kaiserslautern, West-Germany

The feasibility of a novel technique (STIRAP = stimulated Raman adiabatic passage) for efficient and selective population transfer from a thermally populated level 1 via an intermediate state 2 to level 3 is experimentally demonstrated. It is shown for sodium dimers that the process of on- or near resonance stimulated Raman scattering with only partially overlapping laser beams is in particular useful for the selective population of high vibrational levels of particles in a molecular beam. This is achieved when the interaction with the Stokes laser, coupling levels 2 and 3, begins earlier than the interaction with the pump laser. The phenomenon, which is closely related to the formation of "trapped states", is quantitatively explained using the basis of eigenstates of molecules strongly coupled to the radiation fields. The similarity and difference to related techniques such as rapid adiabatic passage phenomena in two level systems (RAP), off-resonant stimulated Raman scattering (OSRS), or stimulated emission pumping (SEP) is discussed.

*) present address: Dept. of Physics, State University of New York, Stony Brook, N.Y. 11794-3800

**) permanent address: Nicolaus Copernicus University, Dept. of Physics, 87 - 100 Torun , Poland

1. Introduction

Molecular beam experiments provide very detailed information about the dynamics of inelastic and reactive collisions [1-3]. The strong reduction of the temperature relevant for the population of molecular levels during the supersonic expansion is successfully exploited in such experiments [4]. As a consequence, the vast majority of these experiments deals with molecules in their vibrational groundstate. Investigation of the effect of initial vibrational excitation in collision dynamics is, however, important for a better understanding of e.g. high temperature combustion media [5] or atmospheric processes under non equilibrium conditions [6]. The attempt to better understand the role of high vibrational excitation on the collision dynamics is hampered by the lack of convenient techniques for the generation of beams with a sufficiently high flux of vibrationally excited molecules.

Crossed beams scattering experiments with highly vibrationally excited molecules were first tried a long time ago [7]. A more systematic approach had to await the development of laser methods [8]. Techniques such as IR excitation [9], off-resonance stimulated Raman scattering (OSRS) [10-13], or pumping of vibrational overtones [14], have been successfully applied in the bulk. Stimulated emission pumping (SEP) [15-16] or population of vibrationally excited levels by spontaneous emission ("Franck-Condon pumping", FCP) [17-21] are other methods now being used in molecular beam experiments as well. Most of these experiments exploit the efficiency and selectivity of IR-excitation to the first vibrationally excited level, v"=1 [22-26]. Population of vibrational levels v" > 1 in beams by SEP holds promise of becoming a routine method [27, 28]. Also, the FCP - method has been used successfully in beams for the measurement of integral [18, 19], as well as differential cross sections [17, 20, 21].

due to limitations imposed by transition probabilities or selection rules. One photon IR excitation and OSRS allow the population of the first vibrationally excited level only. Therefore, systematic experimental study of the variation of the collision dynamics with vibrational excitation is scarce. Up to date, the most complete study of this type is the pioneering work of Toennies and coworkers [18, 19]. Some data recently became available from this laboratory as well [20, 21].

An ideal method should allow efficient and selective population of a large range of vibrational levels in diatomic or polyatomic molecules. In the context of this work, which essentially deals with a modified 3-level system (see Fig. 1), the efficiency E(v",j") is defined as the fraction of the thermal population of the level (v"=0, j"), summed over the orientational quantum number m", which is transferred to an excited level (v", j"). E(v",j") = 1 describes complete population transfer between these levels. The selectivity S(v",j") is given by the ratio of the population transferred to the level (v",j") and the population transferred to all levels in the electronic ground state by the optical process. For S(v",j") = 1 we also have E(v",j") = 1 , if level 1 is completely depopulated and there are no competing processes (see Fig. 1), such as multiphoton ionization or dissociation. Otherwise, we may have E < 1 but still S ≈ 1.

High selectivity S(v",j") is important, in particular, for the study of reactive collision processes. S(v",j") = 1 is furthermore desirable for the investigation of vibrational transitions or collision induced dissociation involving levels v" >> 1. High selectivity of the optical excitation process is not vital e.g. for experiments aiming at the measurement of total integral cross sections in crossed beams experiments [18, 19]. For the latter experiments, the FCP - method has been successfully applied. In this case the selectivity S(v",j") is essentially given by the Franck-Condon factor for the transitions between the level (v',j') in the electronically excited state and the level (v",j").

It has been demonstrated recently, that efficient population of the level v" = 4 of the OH - radical [29] is possible with SEP despite the relatively small Franck-Condon factors for the relevant optical transitions. Vibrational levels of the NO molecules in the electronic ground state as high as v" = 25 have been populated [30] using tunable excimer lasers. An efficiency of the order of E = 0.3 has been reported. Although these experiments demonstrate significant progress towards gaining more complete control over the vibrational degree of freedom in collision experiments, they still suffer from a lack of a high selectivity. Inevitably, a significant fraction of the transient population in the electronic state will be transferred to other vibrational levels by spontaneous emission.

In this paper, we discuss a new laser technique which is based on the stimulated resonance or near-resonance Raman scattering process [31, 32] induced by two partially overlapping laserbeams. This method allows one to combine a very high efficiency with a selectivity S ≈ 1 for the population of levels v" >> 1. The technique can be considered an exceedingly simple version of population transfer by (passive) pulse shaping [33 - 38]. In fact, it has been recognized [39-48] that a high efficiency for population transfer may be achievable with appropriate timing of the interaction with the pump - and Stokes laser. Preliminary results of our approach have been reported previously [49]. These results have been confirmed for three-level systems coupled by IR-radiation field by Reuss and coworkers [50].

Here, the technique is demonstrated for sodium dimers in a molecular beam, interacting with two spatially displaced cw-laser beams. It is shown that the process can be considered as a three-level analogue of the adiabatic passage phenomenon in two-level systems. Adiabatic passage processes in two-level systems have been studied theoretically [51-53] and experimentally [54-56]. Population of e.g. molecular vibrational levels v" = 1 [54] or

complete transfer in atoms has been achieved [56]. Extension to multi-level systems was also considered and experimentally observed [57 - 58]. We propose the name STIRAP - technique (stimulated Raman adiabatic passage) for the corresponding process in a three-level system. We note that it was attempted previously [59, 60] to explore the use of stimulated Raman scattering with cw lasers for the population of high vibrational levels. In those experiments, however, one of the crucial parameters, namely the spatial overlap between the pump and Stokes laser beams, was not varied. The characteristic features of this transfer process are discussed in the framework of the molecular eigenstates dressed by the radiation field [61]. The close relation of our approach to previous work leading to the observation of "trapped states" in three - level systems interacting with two laser fields [62-68] will become obvious. Actually, for the first time, trapped states are observed and experimentally characterized for molecules in this work.

Because of their extraordinary large electronic transition dipol moment (~ 10 debye, [69]) sodium dimers are ideally suited for the exploratory studies reported here. Transition dipole moments of molecules, such as NO or OH, are typically two oders of magnitudes smaller. Presently commercially available cw lasers are not sufficiently powerful for the application of the STIRAP technique to these species. Therefore, the prospects of implementing this method with pulsed lasers will be considered, based on the results from numerical studies, in a forthcoming paper, hereafter referred to as paper II.

In the present paper, we discuss in Sections II, III and IV some general aspects of three-level systems, relevant for this experiment, the experimental set-up and results, respectively. The discussion in Sect. V provides a comprehensive explanation of the observed phenomena. Some features of the STIRAP method are compared to those of other techniques in Sect VI. A brief summary and outlook conclude this paper.

II Processes in a three level system, spectroscopic data and time scales, relevant for this experiment

The population transfer process discussed in this paper is a generic three - level phenomenon. Although the transfer process will be observable in any three-level system, we will focus on the specific example of a Λ-type level system (see Fig. 1) representing a diatomic molecule. In this context, levels 1 and 3 are ro-vibrational levels in the electronic ground state, while level 2 is a level in an electronically excited state. Level 4 comprises all other levels of the electronic ground state, that can be reached by dipole- allowed transitions from level 2. They are not coupled to the laser fields. The population in level 3 is probed by laser-induced fluorescence by excitation with a third laser to level 5 in the electronic state.

The levels 1 and 2 are coupled by the pumplaser, the power, frequency and wavelength, of which are P_p, ν_p and λ_p, respectively. The detuning of the pumplaser frequency from the transition frequency ω_{12} is denoted $\Delta_p = \omega_{12} - \omega_p$. Levels 2 and 3 are coupled by the Stokes-laser. The corresponding quantities carry the index s. Population established in level 2 will decay to the levels k = 1, 3 and 4 with rates A_{2k}. We assume, that there are no additional competing channels such as multiphoton ionization or dissociation leading out of the level system shown in Fig. 1. Radiative decay of levels 1, 3 and 4 is considered to be negligible during the interaction time of the molecules with the laser (in our case less than 200 ns). For a homo-nuclear molecule, radiative decay of level 3 is forbidden [70]. Most data shown below are obtained with the laser frequencies tuned to resonance with the respective one-photon transitions, $\Delta_{p,s} = 0$. Two-photon Raman resonance is established for $\Delta_p - \Delta_s = 0$.

The radiative coupling of two levels is characterized by the Rabi-frequency [71]

$$\Omega(t) = \frac{\mu E(t)}{\hbar} \qquad (1)$$

where μ is the dipole matrix element for the corresponding transition and E is the time dependent field of the laser radiation. When the lasers are detuned from the one-photon resonance, the effective Rabi-frequency is $\Omega(\Delta) = \sqrt{\Omega^2 + \Delta^2}$. The assumption of a periodic modulation of the population of individual levels in the two-level system with a well defined Rabi-frequency implies a sufficiently long coherence length of the radiation [71].

The experimental results discussed below are obtained in the collision free regime of the molecular beam. It is in particular important that the decay rate γ_{13} of the coherence established between levels 1 and 3 is small compared to the inverse of the interaction time of the molecules with the laser beams, $\Delta\tau^{-1}$. The rate of spontaneous decay of levels 1 and 3 as well as the rate of collision processes affecting all levels is negligible on the timescale of the interaction with the lasers [72]. The damping processes that remain operative under our experimental conditions are the radiative decay of level 2, the "time-of-flight relaxation" due to the finite interaction time of the molecules with the laser beams [73], and the effect of the finite coherence length of the lasers.

The spectroscopic data relevant for this particular experiment are summarized in table I. The data for the probe laser which is used to monitor the population established in level 3 is also given in this table. The linestrength factor L for the R-transition used here is L = 0.55 [see e.g. refs. 70, 76 and 77].

Relevant Rabi-frequencies are summarized in Table II. An intensity of $10^5 mW/mm^2$ is obtained for a power of 80 mW focussed to a beam of 170 μm radius (w_b). We note that the interaction time is long

compared to the Rabi-frequency under typical experimental conditions. This implies that perturbation theory treatment of the radiative interaction is not appropriate.

It is also important to realize that under our experimental conditions the interaction time of the molecules, travelling with a speed of u $\approx$ 1000 m/s , with the lasers exceeds the radiative lifetime by about one order of magnitude. Thus, the population in level 1 can be partially or fully depleted by optical pumping before the molecules reach the center of the laser beams [78]. This observation suggests to position the Stokes laser upstream of the pump laser. In such an arrangement the probability of stimulated processes is strong as soon as the molecules interact with the radiation field of the pump laser. In fact, it was argued that lack of flexibility of the spatial displacement of the pump- and Stokes laser beams in previously related experiments [60, 79], prevented us from achieving an efficiency E > 0.75, even under the most favorable conditions. For the population transfer to the level v" = 5, considered here, no more than E = 0.2 was realized in that work [60].

III Experimental

The experimental set-up is schematically shown in Fig 2. The vacuum chamber consists of three segments, the source chamber (typical pressure 10^{-4} mbar), a differential pumping stage (10^{-5} mbar) and the main chamber with the preparation and detection region (10^{-6} mbar). The diameters of the collimating apertures as well as their spatial separation are given in the figure.

The oven is a stainless steel cylinder heated by thermocoax wires to a temperature of about 930 K, which corresponds to a vapor pressure of about P_0^{Na} = 65 mbar. The sodium expands through a nozzle of 0.2 mm diameter together with Ar (P_0^{Ar}=500 mbar) as carrier gas and passes through a heated skimmer. The temperatures

for the translational, rotational and vibrational degree of freedom are about 10 K, 30 K, and 70 K, respectively [80, 81]. At these temperatures the maximum thermal population in the vibrational ground state is found near j" = 5. This level is chosen as level 1. The thermal population of level 3 (v"=5, j") is negligibly small. From previous experiments [80] we conclude that the dimer molefraction is about 20% under these conditions. The flow velocity is $u \approx 10^3$ m/s. From these data we estimate the flux of dimers at the skimmer, the preparation region and at the entrance slit of the detector to be about $2\ 10^{15}$ s^{-1}, $5\ 10^{11}$ s^{-1} and 10^{11} s^{-1}, respectively. About 8% of the dimers are found in the level (v" = 0, j" = 5). The molecules cross the pump- and the Stokes laser at right angles. These laser beams originate from two stabilized single-mode dye-lasers (Coherent 699-21 and 699-29) with a linewidth of the order of 1 MHz. They are transmitted to the apparatus through polarization preserving single- mode optical fibres. The linear polarization as well as a nearly Gaussian intensity profile is maintained. The beams exiting the fibres are collimated with lenses. For both beams, the focus of w_E = 170 μm radius is located at the molecular beam axis. The Rayleigh length [82] is about 140 mm. Thus, in the vicinity of the molecular beam axis, the wave fronts of both beams can be considered, to a very good approximation, as being plane.

The Stokes laser is reflected from the mirror M1 before being superimposed with the pump laser at a dichroic mirror M2. The position of the former is controlled with a micrometer to an accuracy of 10 μm. The small angle of incidence allows accurate control of the spatial separation D of the axes of the Stokes - and pump laser beams. The position of full overlap D = 0 (coinciding laser beam axes), is determined by observing the expanded beam profiles about 1 m beyond the vacuum chamber. The direction of linear polarization of the two lasers is the same.

The detector assembly D1 [77, 83] is located 280 mm downstream from the interaction region with the pump and Stokes lasers. A small circular aperture (0.3 mm diameter) assured that only molecules flying near the molecular beam axis are detected. A third stabilized single-mode laser (Coherent 599-21) is used to induce fluorescence which is collected and transmitted via a fibre bundle to a photomultiplier (Hamamatsu R943-02) outside the vacuum chamber. An auxiliary detector assembly D2, consists of a collecting lens, a fiber bundle and a photomultiplier. It allows us to also monitor the fluorescence from the preparation region.

IV. Experimental Results

A) Raw Data and Normalization Procedure

Typical raw data are shown in Fig. 3. They display both commonly known features of Raman processes and laser-induced fluorescence signals under strong pumping conditions as well as the phenomenon of enhanced population transfer with only partially overlapping pump- and Stokes laser beams. In this particular run, the power of the lasers was 200 mW and the diameter of the beams was 1.5mm. The pump - and Stokes laser axes are coincident for the data shown in Fig. 3a while the optimum displacement D_{opt}, with the Stokes laser preceding the pump laser, is used for Figs. 3b and c. The laser-induced fluorescence is observed with the probe laser frequency tuned to resonance for the transition between the levels 3 and 5 (see Table I and Fig. 1) while the frequency of the Stokes laser is tuned across the 2 - 3 resonance.

The pump laser frequency is tuned almost to resonance ($\Delta_p \approx 0$) with the transition between levels 1 and 2 for the data shown in Fig 3a and 3b, while we have $\Delta_p/2\pi$ = - 240 MHz for Fig. 3c. Level 3 is populated by spontaneous emission from level 2, induced by the pump laser. The interaction of the Stokes laser with the molecules is negligible for detunings exceeding $|\Delta_s|/2\pi$ = 1 GHz. For a

detuning less than the saturation broadened linewidth ($|\Delta_s|/2\pi$ < 400 MHz) the population established in level 3 is depleted by optical pumping. When the two-photon (Raman) resonance $\Delta_p - \Delta_s = 0$ is met, an enhanced population in level 3 is observed for a small range of detuning Δ_s due to the contribution of the stimulated Raman process. This contribution is drastically enhanced for suitably displaced laser beams (see Fig. 3 b).

Due to the large saturation broadened linewidth of the one photon transition, some population is established by spontaneous emission even for pump laser detuning as large as $|\Delta_s|/2\pi$ = 240 MHz (see Fig. 3c). In this case, the maximum depletion of the population by Stokes laser pumping is again observed for $\Delta_s = 0$, while the Raman resonance, leading to efficient population transfer, is observed for $\Delta_s = \Delta_p$. The line shape associated with the optical pumping depletion is a complex function of both laser intensities and the overlap of their profiles. The latter quantity was not controlled when these data were recorded. Therefore, the line shape of the [illegible]etion signal, near $\Delta_s = 0$, seen in Fig. 3, carrie little useful information.

The data of Fig. 3 suggest a convenient method to determine the absolute transfer efficiency E. The power of the pump laser is sufficiently high to deplete the thermal population of level 1 to a negligible level (see e.g. ref. [8], Fig. 12.4). A residual population of less than $5\ 10^{-3}\ n_0$ was routinely assured. The branching ratio B of the spontaneous emission into level 3 is given by $L\ F_{23}$, the product of the linestrength factor L and the Franck-Condon factor F_{23}. The fraction $L\ F_{12}$ of the molecules in level 2 returns to level 1 and can be pumped again. The rates of processes competing with spontaneous emission, such as collisional energy transfer or excitation to higher lying electronic levels or photoionization, are negligible. Therefore, the efficiency of the population transfer without the Stokes laser is given by $B = L\ F_{23} (1 + L\ F_{12})$. From the data of Table I we find B = 0.03. The enhancement V of the population in level 3 due to the stimulated

Raman process compared to the spontaneous emission level B is easily obtained from data such as those given in Fig. 3b. The transfer efficiency as well as the selectivity S = E is then given by $E = B\ V$.

B The Transfer Efficiency

Absolute transfer efficiencies E are shown for $\Delta_p/2\pi = 0$ and $\Delta_p/2\pi$ = 400 MHz in Fig. 4 and 5, respectively as the spatial overlap of the pump laser and Stokes laser beam is varied. The displacement D of the laser beam axes is given in units of the beam waist w_b 170 μm. Typical configurations are depicted in the upper panel of the figures with A, B, and C corresponding to no overlap, optimum overlap and full overlap with coinciding laser beam axes (D = 0), respectively. The molecules interact first with the Stokes laser in configuration A and B, while the pump laser beam axis is placed upstream of the Stokes- laser, partially overlapping the latter, in configuration D.

The Stokes laser is ineffective in configuration A because it interacts with the initially empty levels 2 and 3 before any population is removed from level 1. Therefore, the fraction B = 0.03 of the thermal population of level 1 (see preceding Section) is transferred to level 3 by spontaneous emission. This fraction is monitored by the detector D1 far downstream (see Fig. 2). The dramatic enhancement of the transfer efficiency for optimum overlap ($D_{opt} < 0$, configuration B), with E ≈ 0.95 is obvious. For coinciding beams, configuration C, the efficiency E ≈ 0.2 still exceeds B by a factor of approximately 7. The molecules interact first with the pump laser in configuration D. In this configuration, optical pumping by the Stokes laser or a STIRAP transfer process from level 3 back to level 1 (see Sect. V B4) depletes any transient population in level 3, leading to E = 0.

Fig. 5 shows data similar to those of Fig.4 , however, with pump and Stokes laser detuned by $\Delta_{s,p}/2\pi$ = 400 MHz. This detuning is large compared to the natural linewidth of 12.5 MHz and even exceeds the saturation broadened linewidth, see Fig. 3. The two-photon resonance is still maintained. The excitation efficiency from level 1 to level 3 is significantly reduced because of the large detuning Δ_p from the resonance frequency. Therefore, $E \approx 0$ is observed in configuration A. A transfer efficiency $E > 0.7$ is again observed for optimum overlap, $D_{opt} < 0$. For configuration C the efficiency reduces to $E \approx 0.2$ and reaches another maximum for $D > 0$. The transfer efficiency related to this latter maximum is consistently smaller than the one observed for $D < 0$. The maximum for $D > 0$ appears as soon as the detuning of the lasers, $\Delta_s = \Delta_p \neq 0$, is sufficiently large.

Fig. 6 shows the variation of the transfer efficiency with the detuning Δ_s of the Stokes laser for optimum displacement, D_{opt}, of the beam axes and Δ_p = 0. An efficiency of $E \approx 0.95$ is again observed for Raman resonance $\Delta_p - \Delta_s = 0$. Further data about the variation of the efficiency with Δ_p and Δ_s is summarized in Table III. Although the maximum efficiency E decreases with increasing $|\Delta_p|$, it still exceeds the value given by B (see Section A) for detuning as large as $|\Delta_p|/2\pi$ = 1 GHz.

The width (FWHM) of $E(\Delta_s)$ decreases from about 40 MHz to about 10 MHz with increasing detuning Δ_p. It is this small linewidth which causes the relatively large fluctuations of the observed transfer efficiency (see also Fig. 4 and 5). Even for $\Delta_p = \Delta_s = 0$, the frequency difference between the two lasers must remain constant to within a few MHz, (see Fig. 6). Thus, for optimum performance, each of the two lasers should be stabilized to 1 MHz or better. Active frequency stabilization of both the absolute frequency of the pump laser and the frequency difference between pump and Stokes lasers, based on a novel concept [84], is currently under development in this laboratory. This device will be in operation

in the near future and should lead to significant improvement of the quality of the data and render the STIRAP technique applicable for scattering experiments. However, the quality of the data presented in this work, is fully adequate for the discussion of the features of the STIRAP method as well as a detailed comparison with theory.

We conclude this section by discussing the data of Fig.7, where the fluorescence from the preparation region was observed with the auxiliary detector D2 in parallel with the transfer efficiency. For optimum overlap of the laser beams and Δ_p = 0, Δ_s is tuned across the Raman resonance. As expected, the fluorescence intensity (Fig. 7a) decreases as soon as the transfer efficiency increases (Fig. 7b). The close correlation of this phenomenon as well as those shown in Figs. 4-6 with "dark resonances" and the selective population of "trapped states" [63 - 68] will be discussed in the following Section. The intensity of spontaneous emission does not decrease to zero level because $E < 1$. Furthermore, the auxiliary detector D2 collects light from a large area because no spatial filtering [85] is employed. Thus, fluorescence from molecules crossing the far out wings of the laser beams, where the conditions for efficient population transfers are not satisfied, may also contribute.

V Discussion

It has been emphasized in Section II (see also Table II) that we are dealing with a strong field phenomenon. Therefore, the eigenfunctions $|1\rangle$, $|2\rangle$, and $|3\rangle$ of the molecules are not a convenient basis set for the description of the population transfer process. Rather, the eigenfunctions of the molecules coupled to a strong radiation field (see e.g. [34, 62, 67, 86]), labeled $|a^+\rangle$, $|a^0\rangle$, and $|a^-\rangle$ are preferred. These eigenfunctions, the relevant features of which will be reviewed in Section A, can be expanded in

the basis of the eigenstates $|1\rangle$, $|2\rangle$ and $|3\rangle$ of the molecule in the presence of weak fields $\Omega_{p,s} \approx 0$. Under the conditions of our experiment, the coefficients of this expansion are explicitely time dependent. We consider the case in which particles in a molecular beam interact with cw laser fields. Alternatively, stationary molecules may be exposed to laser pulses. In part B, the time dependence of the coefficients, as well as the conditions for selective population of specific states, will be discussed. Necessary criteria for maintaining the population in these states are given in Part C, while inherent limitations preventing us from realizing the efficiency E = 1 are discussed in Part D.

A. Molecular eigenstates, strongly coupled to radiation fields

The Hamiltonian of a three-level system with states $|1\rangle$, $|2\rangle$ and $|3\rangle$ (see Fig.1) interacting with two laser fields is given by $H_{TOT} = H_{MF} + H$ where $H_{MF} = H_{Mol} + H_{Field}$ combines the Hamiltonians of the free molecule and the radiation fields, while the molecule-field interaction is given by H. Only the latter one is of interest here. It reads, using the rotating wave approximation (see e.g. ref. [52, 58]).

$$H = \frac{1}{2}\hbar \begin{bmatrix} -2\Delta_p & \Omega_p(t) & 0 \\ \Omega_p(t) & 0 & \Omega_s(t) \\ 0 & \Omega_s(t) & -2\Delta_s \end{bmatrix} \qquad (2)$$

The strength of the interaction, given by the Rabi frequencies $\Omega_{p,s}$, see eq.(1), is explicitly time dependent. The time dependence is induced by the directional flow of the molecules through the laser beams or results from the interaction of stationary molecules with laser pulses. The detuning of the laser frequencies from the respective transition frequencies, given by $\Delta_{p,s}$ (see Fig.1), is constant. We restrict the discussion to the case of two photon resonance, $\Delta_s - \Delta_p = 0$, which is the most relevant under our experimental conditions. We note, that radiative decay

and collisional damping are not included explicitly in H. The consequences of this fact will be discussed below.

It is easy to verify [44, 62, 64] that

$$|a^0\rangle = \cos\Theta\,|1\rangle - \sin\Theta\,|3\rangle \qquad (3)$$

with $\tan\Theta = \Omega_p/\Omega_s$, or

$$\sin\Theta = \frac{\Omega_p}{\sqrt{\Omega_p^2 + \Omega_s^2}} \quad \text{and} \quad \cos\Theta = \frac{\Omega_s}{\sqrt{\Omega_p^2 + \Omega_s^2}} \qquad (4)$$

is an eigenfunction of H, eq(2), i.e. of the three-level system coupled to the radiation fields.

The eigenfunction given by eq.(3) is of particular importance. It includes no contribution from the intermediate level 2, i.e. we have $\langle 2|a^0\rangle = 0$.

It can furthermore be verified that the other two eigenfunctions are

$$\begin{aligned} |a^+\rangle &= \sin\varphi\sin\Theta\,|1\rangle + \cos\varphi\,|2\rangle + \sin\varphi\cos\Theta\,|3\rangle \\ |a^-\rangle &= \cos\varphi\sin\Theta\,|1\rangle - \sin\varphi\,|2\rangle + \cos\varphi\cos\Theta\,|3\rangle \end{aligned} \qquad (5)$$

The eigenvalues of $|a^{\pm}\rangle$ and $|a^0\rangle$ are

$$\begin{aligned} \lambda^{\pm} &= -(1/2)\left(\Delta_p \mp \sqrt{\Delta_p^2 + \Omega_p^2 + \Omega_s^2}\right) \\ \lambda^0 &= -\Delta_p \end{aligned} \qquad (6)$$

The angle Θ is given by

$$\tan\Theta = \frac{\sqrt{\Omega_p^2 + \Omega_s^2}}{\sqrt{\Omega_p^2 + \Omega_s^2 + \Delta_p^2} - \Delta_p} \qquad (7)$$

The variation of the eigenvalues $\lambda^{0,\pm}$ with the reduced time $\tau = t/\Delta\tau$ is shown in Fig. 8 for on-resonance and off-resonance pumping, $\Delta_p = 0$ and $\Delta_p \neq 0$, respectively. Here, $\Delta\tau$ is defined by $\Omega_{p,s}(t) = \Omega^0_{p,s}\, e^{-\left[\frac{t}{\Delta\tau}\right]^2}$.

If the eigenfunctions of the full Hamiltonian H_{TOT} are of interest, the photon numbers n_p and n_s need to be considered. Instead of $|a^{0,\pm}\rangle$ we then have $|a^{0,\pm}, n_p, n_s\rangle$, the so called dressed states [34, 61, 62]. The variation of the laser fields is, however, not of interest here. Therefore, n_p and n_s are omitted.

B. Selective Population of the States $a^{0,\pm}\rangle$

The wavefunction of the molecule, coupled to the radiation fields, can be written as

$$|\psi(t)\rangle = a^+|a^+(t)\rangle + a^0|a^0(t)\rangle + a^-|a^-(t)\rangle. \qquad (8)$$

The eigenstates $|a^{0,\pm}(t)\rangle$ are time dependent because the molecules propagate through the laser fields, characterized by $\Omega_{p,s}(t)$. Furthermore, the coupling between these eigenstates due to non-adiabatic transitions can be calculated from the time dependent Schrödinger equation. Thus, the coefficients $a^{0,\pm}$ may be time dependent as well.

Without collisional or radiative damping which lead to the population of the levels 4 or for $t \to -\infty$, we have

$$(a^+)^2 + (a^0)^2 + (a^-)^2 = 1. \qquad (9)$$

The state $|a^0\rangle$ is formed by a coherent superposition of state $|1\rangle$ and $|3\rangle$. Selective population of this particular state requires $a^0 = 1$, and $a^\pm = 0$. Before interaction with the lasers (i.e. for $t \to -\infty$) the molecule is in the state $|1\rangle$. If it emerges in the eigenstates $|a^0\rangle$ and the evolution of $|\psi(t)\rangle$ is adiabatic, the molecule is "trapped" in this state, since it is not affected by properties of the intermediate level 2. In particular, this state is not affected by damping due to spontaneous decay. If the unstable states $|a^+\rangle$ or $|a^-\rangle$ are populated, the molecules will decay to the levels 4, due to spontaneous emission. The decay rate depends on the value of $|\langle 2|a^+\rangle|$ or $|\langle 2|a^-\rangle|$, given by the mixing angle ϕ.

3.1 Selective population of $|a^0\rangle$, $D < 0$.

Inspection of eq.(3) reveals a straightforward and the surprisingly simple recipe for the selective population of the stable state $|a^0\rangle$. If $\Omega_s \gg \Omega_p$ is valid for $t \to -\infty$ but $\Omega_p \gg \Omega_s$ for $t \to +\infty$, we have $\cos\Theta \approx 1$ for early times, but $\sin\Theta \approx 1$ at later times. Thus, when the Stokes laser precedes the pump laser, we have $|\langle 1|a^0\rangle| \approx 1$ at early times, which implies a vanishingly small probability for the population of the "unstable" states $|a^+\rangle$ and $|a^-\rangle$. It is only through the decay of these unstable states that the population could leak out of the three - level system into level 4, see Fig.1. These conclusions are also valid when the laser frequencies are detuned from the one-photon resonance, i.e. $\Delta_{p,s} \neq 0$, because the mixing angle Θ does not depend on Δ_p.

B 2 Population of $|a^{\pm}\rangle$, D = 0.

It is instructive to consider the mixing angle Θ, see eq.(3), for overlapping fields. When the axes of the laser beams overlap and the shape of the beam profiles is identical, the ratio of the Rabi frequencies and thus the mixing angle Θ does not vary in time, see eq.(4). For instance, for $\Omega_p = \Omega_s$ we have $\cos\Theta = \sin\Theta = 1/\sqrt{2}$ leading to $|\langle 1|a^0\rangle|^2 = 0.5$. Thus, only 50% of the initial population of level $|1\rangle$ emerges in the stable state $|a^0\rangle$ the rest will be shared between $|a^+\rangle$ and $|a^-\rangle$ depending on the detuning Δ_p.

For $\Delta_p = +\omega$ only 50% of the population of $|a^0\rangle$ will be found in state $|3\rangle$, because we have $|\langle a^0|3\rangle|^2 = 0.5$. For $\Delta_p = 0$, most of the population in $|a^{\pm}\rangle$ is lost by radiative decay and the transfer efficiency is $E = |\langle 1|a^0(t = -\infty)\rangle|^2 \; |\langle a_0(t = +\infty)|3\rangle|^2 = 0.25$. In fact, $\Omega_p = \Omega_s$ was assumed in the numerical calculations (see also Ref. [49], Fig. 2,) and is approximately valid in the experiment (see Fig.4 and 5). Numerically and experimentally a transfer efficiency $E \approx 0.25$ was indeed found for D = 0 and $\Delta_p = 0$.

B3 Selective Population of $|a^{\pm}\rangle$, D > 0.

The transfer efficiency E for the configuration D > 0 (pump laser preceding Stokes laser), varies from E = 0 to $E \lesssim 1$ with increasing detuning Δ_p, see Fig. 4 and 5. For D > 0 we have initially $\Omega_p \gg \Omega_s$ leading to $\cos\Theta \ll 1$ and only a negligible fraction of the thermal population n_0 in state $|1\rangle$ emerges into the stable state $|a^0\rangle$ since $\langle 1|a^0\rangle \approx 0$, see eq. (3). Thus only the unstable states $|a^{\pm}\rangle$ will be populated. From eqs. (4-6) we find $\tan\phi = 1$ for on-resonance pumping, $\Delta_p = 0$. The mixing angle $\phi = 45°$ implies that both states $|a^{\pm}\rangle$ are equally populated.

For off-resonance pumping, $|\Delta_p| \neq 0$, the states $|a^{\pm}\rangle$ are again populated, although unevenly. Using eqs. (4) and (5) in eq. (6)

for large positive detuning, $\Delta_p^2 \gg \Omega_p^2 + \Omega_s^2$ we find for $\Delta_p > 0$ $\tan\phi \approx 2\,\Delta_p/\sqrt{\Omega_p^2+\Omega_s^2}$ or $\phi \approx 90°$. Therefore, we have initially $|\langle 1|a^+\rangle| \approx 1$ and $|\langle 1|a^-\rangle| \approx 0$ but also $|\langle 2|a^+\rangle| \approx 0$. The population emerges almost completely into state $|a^+\rangle$, with little contribution of the intermediate level. At later times $|\langle 3|a^+\rangle|$ approaches unity and efficient population transfer is again possible. Thus, for very large detuning $\Delta_p > 0$ the state $|a^+\rangle$ develops the same character as the stable state $|a^0\rangle$. For $\Delta_p < 0$ the population transfer occurs via the state $|a^-\rangle$.

B4 Evolution in time and summary of Part B

Fig. 9 shows the population ρ_{ii} of levels i as a function of the reduced time $\tau = t/\Delta\tau$ as obtained by numerical solutions of the corresponding density matrix equations in rotating wave- and slowly varying envelope approximation. A maximum local Rabi frequency $\Omega^0_p = \Omega^0_s = 10^9\ s^{-1}$ at the axes of the laser beams with a power of about 80 mW and a waist of 170 μm was assumed. The transit time of the molecules travelling along the molecular beam axis with 1000 m/s across the laser beams is 170 ns. Spontaneous decay of level $|2\rangle$ (lifetime 12.5 ns) has been included in the calculation. The smooth and complete transfer of population from state $|1\rangle$ to state $|3\rangle$ for optimum displacement is obvious. For complete overlap, D = 0, the maximum transient population of the intermediate state, level 2 is as large as 10% while it does not exceed 10^{-3} for D_{opt}.

It is interesting to note, that a STIRAP process is also discernible for D > 0, pump laser preceding the Stokes laser, see Fig. 9 right hand side. The pump laser depletes the population of level 1 and populates level 3 by spontaneous emission. This process is essentially completed at $t = -2\Delta\tau$. Therefore, the molecules enter the overlap region with some population in level 3 but no population in level 1 and population transfer back to level 1 occurs.

This is demonstrated by the insert. Thus, it is not the process of optical pumping but the "reverse" STIRAP- process that leads to a complete population depletion of level 3 for $\Delta_p = 0$ and $D > 0$, see also Fig. 4.

The flow of the population from the initially populated level $|1\rangle$ via the states $|a^{0,\pm}\rangle$ into the level $|1\rangle$ and $|3\rangle$ is schematically shown in Fig. 10 for the various combinations of displacement D and detuning Δ_p. The wide and small arrows indicate fast and slow damping of the states $|a^{\pm}\rangle$ through radiative decay, respectively. Further details are given in the figure caption.

Summarizing the conclusions from part B, we realize that the "counter intuitive" arrangement of the Stokes and pump laser assures smooth transfer of the molecules from state $|1\rangle$ to state $|3\rangle$ by selective population of $|a^0\rangle$. In a sense the Stokes field, which couples the initially unpopulated levels 2 and 3, prepares the molecule for a smooth transfer of population from level 1 to 3 upon interaction with the pump laser.

C Criteria for Adiabatic Evolution

We recall that the evolution of the wavefunction $|\psi(t)\rangle$ of the molecule is determined by the Schrödinger equation. For given laser intensities, or Rabi frequency $\Omega_{p,s}$, and location in the beams, the states $|a^{0,\pm}\rangle$ (eqs. 3 - 5) are eigenstates of the molecules coupled to the radiation fields. Since the Hamiltonian H, eq. (2), is explicitly time dependent, the rate of change of H(t) determines whether or not coupling between the states $|a^{\pm,0}\rangle$ is vanishing small as the molecules propagate through the laser beams. If the adiabatic following condition is satisfied throughout the interaction time between the molecules and the fields and if the molecules are initially placed into e.g. state $|a^0\rangle$, i.e. if

$$|\psi(t)\rangle \approx |a^0(t)\rangle \tag{10}$$

is valid at early times, eq. (10) is valid also at later times and the time evolution of the population transfer between the states $|1\rangle$ and $|3\rangle$ is given by eq.(3).

It is well known that adiabatic evolution of the states is assured when the rate of nonadiabatic coupling is small compared to the separation of the corresponding eigenvalues [88], see Fig. 8, i.e. when

$$\left|\langle a^{\pm} \left|\frac{d}{dt}\right| a^0\rangle\right|^2 \ll \left|\omega^0 - \omega^{\pm}\right|^2 \tag{11}$$

It is easy to show, using eqs.(3) and (5) that $\left|\langle a^{+}\left|\frac{d}{dt}\right|a^0\rangle\right|^2 + \left|\langle a^{-}\left|\frac{d}{dt}\right|a^0\rangle\right|^2 = \left|\frac{d\Theta}{dt}\right|^2$. Adiabaticity is maintained when the rate of change of the mixing angle Θ is sufficiently small, i.e. when

$$|\dot{\Theta}| \ll |\omega^0 - \omega^{\pm}| \tag{12}$$

is valid. This criterion is evaluated for particles in a molecular beam propagating through spatially displaced laser beams.

From eq.(4) we find the rate of change of the mixing angle to be

$$|\dot{\Theta}| = \left|\frac{\dot{\Omega}_p\,\Omega_s - \Omega_p\,\dot{\Omega}_s}{\Omega_p^2 + \Omega_s^2}\right| \tag{13}$$

We also assume that the intensity profile of the laser beams, as experienced by the molecules travelling with the velocity u through the fields, is reasonably well approximated by

$\Omega_{p,s}(\tau) = \Omega^0_{p,s}\, e^{-(\tau \pm \eta)^2}$ with the reduced variables $\tau = t/\Delta\tau$ and

$\eta = 0.5\, D/(u\,\Delta\tau)$. (14)

The + and − sign apply to the pump and Stokes laser, respectively. From eqs.(13) and (14) we find for $\tau = 0$, the center of the overlap region where the rate of change of $\Theta(\tau)$ is largest,

$$|\dot{\Theta}| = \frac{2\eta}{\Delta\tau} \tag{15}$$

On the other hand we have (see eq. (6))

$$|\omega^0 - \omega^{\pm}| = \sqrt{\Omega_p^2 + \Omega_s^2} \quad \text{for } \Delta_p = 0 \tag{16}$$

and

$$|\omega^0 - \omega^{\pm}| \geq \frac{1}{4} \frac{\Omega_p^2 + \Omega_s^2}{\Delta_p} \quad \text{for } \Delta_p^2 >> \Omega_p^2 + \Omega_s^2 \tag{17}$$

which leads for $\Omega_p = \Omega_s = \Omega^0$ and $\tau = 0$ to

$$|\omega^0 - \omega^{\pm}| = \Omega_0 q(\Omega_0, \eta, \Delta_p)$$

with $q = \frac{1}{\sqrt{2}} e^{-\eta^2}$ and $q = \frac{1}{2}\frac{\Omega_0}{\Delta_p} e^{-2\eta^2}$ for $\Delta_p = 0$ and $|\Delta_p| >> \Omega^0$, respectively.

The optimum displacement of the laser beam axes for maximum transfer efficiency is found for $\eta \approx 0.5$. Thus, we find using eqs. (15-17) and eq.(12) that adiabaticity is maintained in the center of the overlap region, if

$$\Omega^0 \Delta\tau >> F \tag{18}$$

with

$F = 1$ for $\Delta_p = 0$ and $F = \frac{\Delta_p}{\Omega^0}$ for $|\Delta_p| >> \Omega^0$

Higher laser power is needed for efficient population transfer under off-resonant pumping conditions. On the other hand, when E≈1 is achieved for on-resonance pumping, a high transfer efficiency

can be maintained when $|\Delta_p|$ increases as long as eq. (18) is satisfied.

The Rabi frequencies under typical conditions for our experiment (P = 80 mW, w_0 = 170 μm, transitions specified in Table I) are of the order of 10^9 s^{-1}. With u = 1000 m/s, we find $\Omega^0\Delta\tau$ = 170. Thus, for parameters typical for this experiment, the adiabatic following condition is very well satisfied. Molecules that do not cross the laser beam axes are exposed to weaker fields and the relevant Rabi frequencies are reduced accordingly. Nevertheless, a transfer efficiency of E ≈ 1 will be effective, as long as eq.(18) is satisfied. Particles, crossing the laser beam axes not exactly at right angle will experience a Doppler shifted laser frequency. The maximum shift $k_p \cdot v$ (v = the velocity component parallel to the laser beam axes) which is tolerable without reducing E increases with increasing $\Omega^0 \Delta\tau$.

These observations are in particular important for the application of the STIRAP technique to scattering experiments. When eq.(18) is satisfied by a sufficiently large margin, all molecules in level 1 that cross a scattering region with a typical diameter of about 1 mm^2 can be efficiently and selectively excited to level 3.

D Limits of the transfer efficiency E

In this paragraph we mention inherent limitations preventing one from reaching an efficiency of exactly unity.

For a given displacement of the laser beam axes $\eta < 0$, we have $\Theta(\tau = -\infty) = 0^0$ and $\Theta(\tau = +\infty) = 90^\circ$ leading to $|\langle 1|a^0(\tau=-\infty)\rangle|^2 |\langle a^0(\tau=+\infty)|3\rangle|^2 = 1$. However, this does not necessarily lead to E = 1 because for $|\tau| \to \infty$, eq.(12) is not satisfied since $|\omega^0 - \omega^+|$ decreases more rapidly with increasing $|\tau|$ than does $|\dot{\Theta}|$. The maximum transfer efficiency is determined by the

mixing angle $\Theta(r^*)$ at that position or time r^* when eq.(12) is satisfied and the system "locks" into the state $|a^->$. Therefore, an upper limit of the efficiency is given by

$$E_{max} = |\langle 1|a^w(r^*_<)\rangle|^2 \, |\langle a^w(r^*_>)|3\rangle|^2 \tag{19}$$

or

$$E_{max} = \cos^2 \Theta(r^*_<) \sin^2 \Theta(r^*_>) \tag{20}$$

where the adiabatic evolution is assured for $r^*_< < r < r^*_>$. The smaller $\Theta(r^*_<)$ and the larger $\Theta(r^*_>)$, the larger is E_{max}.

The efficiency will increase with increasing $\Omega_{p,s}$ for given separation η of the beam axes. For given $\Omega_{p,s}$ but increasing η the value of $\Theta(r^*_>)$ decreases and $\Theta(r^*_>)$ increases, leading to a larger E_{max}. However, with increasing η, eq.(12) is less likely to be satisfied (see eq.(16) and (17)) in the center of the overlap region, $r = 0$. Consequently, the transfer efficiency E may decrease due to nonadiabatic coupling to the states $|a^+>$ as shown in Fig. 11 for on-resonance pumping . For $\Delta_p = 0$, and using eqs(6), (13) and (14) we numerically determine the value of $r^*_<$ and $r^*_>$ for which we have $|\dot{\Theta}| = z|\omega^w - \omega^+|$ with the somewhat arbitrary choice $z = 5$. E_{max} is then determined from eq.(20).

Also shown in Fig. 11 is the result of the evaluation of the adiabaticity criterion, eq. (12), for $r = 0$. With $|\omega^w - \omega^\pm| = \Omega^w\, g\,(\eta, r, \Delta_p)$ and $|\dot{\Theta}| = h\,(\eta, r)/\Delta r$ we find instead of eq. (18)

$$\Omega_0 \Delta r >> F(\eta, r, \Delta_p)$$

with $F = h/g$. For given Ω_0 and Δr, adiabatic following is maintained, as long as $F(\eta, r, \Delta_p) < F^*$. The variation of F/F^* with η is shown in Fig. 11 for $r = 0$ and $\Delta_p = 0$ with the somewhat arbitrary choice $F^* = 5$. We have $E \approx E_{max}$ as long as $F/F^* < 1$. For $F/F^* > 1$, the transfer efficiency is reduced due non adiabatic coupling to the states $|a^\pm>$ around $r = 0$. Fig. 11 shows that the transfer efficiency remains small for small displacement $\eta << 1$ because of a reduced selectivity in the population of the state $|a^0>$ at early times $r \approx r^*$, while for $\eta > 1$ an efficiency $E < 1$ results from nonadiabatic coupling at $r \approx 0$.

The transfer efficiency E is insensitive to radiative decay or other loss processes from the intermediate level 2. This is true for the optimum configuration $D_{opt} < 0$ and as long as no other damping processes are relevant. In fact the maximum transient population established in level 2 is $< 10^{-3}$ of the thermal population n_0 in level 1 (see Fig.9). This implies that dissociating electronic states could be used as the intermediate level 2, the purpose of which is merely to provide the coupling between the levels 1 and 3 via the Raman process rather than to temporarily store population. However, radiative decay of levels 1 and 3, collisional processes affecting these levels and the coherences in the system and phase fluctuations of the laser beams will reduce the efficiency E.

VI Comparison with other concepts or techniques

A Adiabatic passage and π-Pulse method

It is instructive to compare features of the STIRAP technique with those of other methods. For instance, population inversion can be achieved in a two-level system by an adiabatic passage process or the π - pulse approach [51, 52, 76]. These phenomena are conveniently described in the Bloch-vector model, a powerful tool for

the analysis of coherent processes in two or multi level systems. In the Bloch-vector model the two-level system is characterized by the state vector $\vec{\rho}(t) = (\rho_x(t), \rho_y(t), \rho_z(t))$ with the dispersion, absorption and difference of population $(n_2 - n_1)/(n_1 + n_2)$ being proportional to the x-, y-, and z- components, respectively. The laser field is characterized by the vector $\vec{F}(t) = (-\Omega(t), 0, \Delta(t))$. The evolution of $\vec{\rho}(t)$ in time is given by [52]

$$d\vec{\rho}(t)/dt = \vec{F}(t) \times \vec{\rho}(t) \qquad (21)$$

Initially the normalized state vector is $\vec{\rho} = (0,0,-1)$. For detuning $\Delta = 0$, the field vector $\vec{F}(t)$ evolves parallel to the x-axis. Thus, the two vectors are at right angle and $\vec{\rho}(t)$ precesses around $\vec{F}$ in the y-z plane (see Fig. 12a). This motion of the state vector shows clearly the Rabi oscillations. Complete inversion, $\rho(t) = (0,0,+1)$, is reached at a well defined time t_π given by $\Omega\, t_\pi = \pi$ if Ω is constant or when the variation of $\Omega(t)$ is controlled in such a way to yield $\pi = \int_{-\infty}^{+\infty} \Omega(t)dt$. Realization of such a π -pulse requires careful control of the evolution of the Rabi-frequency (see eq. (1)). For a given shape of $\Omega(t)$ a π-pulse can be realized only for a specific transition dipol moment μ [38]. As a consequence for a realistic system with $j'' > 0$ population inversion can be achieved for only one of the degenerate m''- levels.

A more practical scheme for achieving population inversion in a two-level system is the adiabatic passage technique (see e.g. ref. [51, 54-57, 89]), where $\Omega(t)$ is usually held constant, while the detuning $\Delta(t)$ evolves in time from e.g. negative to positive detuning with $|\Delta(t^*)| >> \Omega$ for $t^* = \pm \infty$. The consequences are obvious from Fig. 12b. The angle between $\vec{F}(t = 0)$ and $\vec{\rho}(t = 0)$ is

small and $\vec{\rho}$ precesses around $\vec{F}$, according to eq.(21), with the effective Rabi frequency $\Omega_{eff} = \sqrt{\Omega^2 + \Delta^2}$. As soon as the detuning is reduced, the angle between $\vec{F}$ increases. If the coupling between these two vectors is sufficiently strong, the vector $\vec{\rho}$ follows $\vec{F}$ adiabatically by evolving along a small precession cone, the axis of which coincides with $\vec{F}$. At later times the state vector approaches $\vec{\rho} = (0,0,+1)$, corresponding to complete inversion of population. Decay processes of level 2 with the rate γ_2 will not interfere as long as the sweep time Δt is sufficiently rapid, $\Delta t << \gamma_2^{-1}$.

Extension of this model to a three-level system discussed in this paper requires, in principle, the representation of the Bloch-vector in higher dimensions [90]. Hioe and Carroll [46] have shown how to reduce the problem to three dimensions for $\Delta = 0$. For large detuning, $|\Delta_p| >> \Omega$ the system can be reduced to an effective two level system [57, 58]. Only this case is discussed here. Grischkowski et al. [58] have shown that for large detuning Δ_p the vector F has the form

$$\vec{F} \sim \frac{1}{4\Delta_p}\,(-\Omega_p\,\Omega_s,\ 0,\ \Omega_p^2 - \Omega_s^2) \qquad (22)$$

We consider the motion of $\vec{F}$ and $\vec{\rho}$ for spatially displaced laser beams. The variation of F_x and F_z is shown in Fig. 12c . The former is given by the product of the Rabi frequencies, which is initially very small. The component F_z, however, is initially dominated by $\Omega_s^2(t)$, which is large as soon as the molecule interacts with the Stokes laser. Therefore, the angle between $\vec{F}$ and $\vec{\rho}$ is initially very small. As the molecules propagate through the laser beams, F_x increases before decreasing again while F_z changes

sign. The time evolution of $\vec{F}$ is shown in Fig. 12d. Provided that the coupling between $\vec{\rho}$ and $\vec{F}$ is sufficiently strong, i.e. if $\Omega_{eff} >> |\dot{\Delta}|$, the state vector follows $\vec{F}$ adiabatically by evolving along a small precession cone, the axis of which coincides with F, just as in the case of the two-level system .

In this STIRAP concept, no active frequency sweep is required in order to induce the adiabatic following process. Merely, the time evolution of the Rabi frequencies, controlled by the intensity variation of the laserfields, is important. In contrast to the rapid adiabatic passage processes in a two-level system, the interaction time of the molecules with the laser needs not to be small compared with the decay of the level 2, since this level is not significantly populated during the STIRAP - process. Rather, the decay of levels 1 and 3 should be sufficiently slow, a requirement easily satisfied for vibrational levels of particles in molecular beams.

One may speculate that sequential application of two π-pulses for the transition between levels 1 and 2 and level 2 and 3 may be feasible and useful for efficient population transfer between levels 1 and 3, as well. We emphasized, however, that population inversion can only be achieved for carefully controlled time evolution of the field, when the π-pulse technique is applied. When a high transfer efficiency is in fact realized for molecules in a specific state (v'', j'', m_0'') travelling with a specific velocity u, then molecules in levels $m'' \neq m''_0$ or travelling at velocities $v \neq u$, will not experience complete population inversion. In contrast, the STIRAP-approach for a three-level system allows one to achieve population inversion for <u>all m" - levels</u>, provided the adiabaticity criterion, eq.(18), is satisfied for the transition with the smallest transition dipol moment. Also, the inversion process is insensitive to a variation of the interaction time of molecules with the laser beams and/or the intensity or shape of the latter.

<u>B Off-resonance Raman Pumping (OSRS)</u>

Off-resonance stimulated Raman scattering (OSRS) is a well established technique for the population of rotational levels in the first vibrational level of the electronic groundstate [10-13]. At first glance the STIRAP method seems to merge into the OSRS process for very large detuning. However, for very large Δ_p, the evolution of level populations can no longer be treated by a three- level model. Unlike for STIRAP the detuning Δ_p from level 2 is no longer small compared to the detuning from other levels also accessible by dipol transitions from level 1. When these levels are included, the matrix of the Hamiltonian, eq.(2), increases in size and the eigenfunctions are no longer given by eqs. (3) and (5). Superposition of all the relevant contributions restricts the vibrational quantum number of accessible levels 3 to $v_3 = v_1 \pm 1$ [91]. A well defined Rabi frequency no longer exists and the coherences are damped. Therefore, coherence properties of the lasers are no longer important when applying the OSRS method and broad band lasers can be successfully used.

<u>C Stimulated Emission Pumping (SEP)</u>

Some features of the STIRAP technique are distinctively different from those of the well known SEP method [15, 16, 29, 30]. Most importantly, the transient population of level 2 is negligible when the STIRAP method is applied, while generic stimulated emission pumping requires a significant population in level 2. SEP is routinely applied with broadband pulsed lasers. Thus, 2 photon-coherences are damped. They are usually neglected, and the population transfer can be treated using the rates for absorption as well as for stimulated and spontaneous emission. For a sufficiently long radiative lifetime, SEP is conveniently applied by firing the pump laser earlier than the Stokes laser with no overlap between the two. When saturation occurs 50% of the population n_0 in level 1 will end up in level 2. Disregarding any deviation of the ratio of degeneracy factors from unity, the Stokes laser will

transfer half of these molecules (i.e. 25% of n_0) into level 3, while 0.5 n_0 will be distributed over all levels by spontaneous emission. When both lasers are fired at the same time and the Rabi frequencies are equal, about 1/3 of n_0 can be transferred to level 3. This is consistent with recent experimental results obtained with high power broad band pulsed lasers [29,30]. If the bandwidth of these lasers were always down to the transform limit, coherent phenomena would become important. Under these conditions SEP would be the same as STIRAP with overlapping laser beams, D = 0, and Δ_p = 0. The most efficient population transfer using STIRAP is, however, achieved for D < 0, or when the Stokes laser is fired earlier than the pump laser.

VII Conclusion

We have demonstrated and analyzed a novel concept (STIRAP) for efficient and selective population of molecular vibrational levels using the stimulated Raman process with only partially overlapping laser fields. The specific timing of the interaction sequence is crucial. The interaction with the Stokes laser should precede that with the pump laser, provided there is sufficient overlap between the two. With STIRAP, the efficiency of the population transfer from an initially populated level to an unpopulated one may approach unity. This method is in particular promising for molecular beam experiments since all molecules in a thermally populated level that fly through a scattering region of a typical size will undergo the transfer process. The population of all degenerate levels (e.g. all m_j-levels of a rotational state) may be transferred at the same time. Furthermore, the efficiency is not very sensitive to experimentally controllable parameters such as the flow velocity u, the laser power P, the frequency detuning Δ_p and details of spatial profile or pulse shape for cw or pulsed lasers, respectively. The population transfer by the STIRAP method is also insensitive to damping processes affecting the intermediate level, such as intra-molecular transfer in polyatomic molecules. The technique can be applied in the bulk as well as long as the collision rates γ_{ik} are small enough, $\gamma_{ik}\ \Delta\tau \ll 1$. Criteria

specifying the conditions for efficient transfer were presented and the features of the STIRAP method were compared with those of other techniques.

We emphasize that some restrictions apply. Coherence phenomena are important in the STIRAP concept. Therefore single mode cw lasers with negligible phase fluctuations during the interaction time $\Delta\tau$ or pulsed lasers with nearly transform limited radiation are needed. Coherent processes are conveniently described in the Bloch vector picture (see Sect VI A). We note that there are many routes of the state vector $\vec{p}(t)$ in the Bloch vector model leading to population inversion. The route imposed on the state vector $\vec{p}(t)$ by the STIRAP method seems to be the most relevant one when implemention of this technique for collision dynamics experiments is considered. We also note that, in the concept of the "optimum control" of Rabitz et. al. [33], our approach may be considered as an exceedingly simple method of passive pulse shaping.

The transition dipol moments of many molecules of interest are too small for successful application of the STIRAP technique. Currently available cw lasers are not powerful enough to induce a sufficiently large Rabi-frequency for transitions between the relevant levels for many of these molecules and the condition given by eq. (18) are difficult to meet. Therefore, it is of significant interest to explore the feasibility of this method when pulsed lasers are involved. This will be done in paper II [92], based on numerical results. In that paper, further numerical results as to the dependence of the transfer efficiency E on the various parameters, such as Rabi-frequency, detuning, separation of the laser beam axis and collision rates will be presented. Furthermore, it will be shown that the STIRAP method can be conveniently used to prepare aligned molecules in levels v" > 1.

Acknowledgement

This work has been supported by the Deutsche Forschungsgemeinschaft through SFB 91 "Energy transfer in atomic and molecular collisions". We thank F.T.Hioe and J.R.Kuklinski for enlightening discussions concerning the evolution of population in a three-level system coupled to strong radiation fields and A. Kuhn for assistance in taking the data of Figs. 3 and the calculation of the data shown in Fig. 9. Finally we thank L. Meyer and R. Walther for their skillful technical assistance.

References

1) R.D.Levine and R.B.Bernstein " Molecular Reaction Dynamic and Chemical Reactivity", Oxford University Press, New York, 1987

2) R.B. Bernstein "Chemical Dynamics via Molecular Beam Techniques", Clarendon Press, Oxford (1980)

3) "Atomic and Molecular Beam Methods", G.Scoles ed. , Oxford University Press, 1988

4) see ref 3, Chapter 2

5) J.A. Campbell "Energy and the Atmosphere" John Wiley & Sons, New York (1977)
K.Kleinermanns and J.Wolfrum Angew.Chem. 99, 38 (1987)
J.Wolfrum in "Selectivity in Chemical Reactions" ed. J.C.Whitehead, Kluwer (1988) p.23

6) T. Slanger, C.E. Jasinski, G. Black, G.E. Jadd Science 241, 945 (1988)
M. Capitelli in "Nonequilibrium Vibrational Kinetics", Topics in current physics, Vol. 39, ed. M. Capitelli, Springer Verlag, New York (1986)

7) F.F. Crim, M.S.Chou, and G.A. Fisk Chem. Phys. 2, 283 (1973)

8) see ref.3, Chapter 12

9) M. Kneba and J. Wolfrum, Ann. Rev. Phys. Chem. 31, 47 (1988)
M.Quack Adv.Chem.Phys. 50, 395 (1982);
D.W.Lupo and M.Quack Chem.Rev. 87, 181 (1987)
J. Wolfrum Laser Chem. 9, 171 (1988)

10) P.Esherick and A.Owyoung, and J. Pliva Chem.Phys.83, 3311 (1985)

11) B.J. Orr, A.B. Duval, P. Haines, N.R. Isenor, and D.A. King J. Opt. Soc. Am. B1, 503 (1984)
B.J. Orr, J.G. Haub, and R. Haines Chem. Phys. Lett 107, 168 (1984)

12) W.Meier, G.Ahlers, and H.Zacharias J.Chem.Phys. 85, 2599 (1986)

13) R.L.Farrow and D.W.Chandler J.Chem.Phys. 89, 1994 (1988)

14) F.F.Crim Ann.Rev.Phys.Chem. 35, 657 (1984)

15) C.Kittrell, E.Abramson, J.L.Kinsey, S.A.McDonald, D.E.Reisner, R.W.Field, and D.H.Katayama J.Chem.Phys. 75, 2056 (1981)

16) C.H.Hamilton, J.L.Kinsey, and R.W.Field Ann.Rev.Phys.Chem. 37, 493 (1986)

17) K.Bergmann, U.Hefter, and J.Witt J.Chem.Phys.72, 4777 (1980);
E.Gottwald, A.Mattheus, and K.Bergmann J.Chem.Phys 86, 2680 (1987)

18) Fuchs and J.P. Toennies J.Chem.Phys. 85, 7062 (1986)

19) H.-G.Rubahn and J.P.Toennies J.Chem.Phys. 89, 278 (1988);
H.-G.Rubahn and J.P.Toennies Chem.Phys. 126, 7 (1988)

20) G.Ziegler, S.V.K.Kumar, P.Dittmann, and K.Bergmann Z.Phys.D 10, 247 (1988)

21) G. Ziegler, S.V.K.Kumar, A.Kuhn, Benfan Sun, and K.Bergmann "Angular resolved rotational energy transfer in high vibrational states: Na2(v"=31) - Ne " to be published

22) J.Odiorno, P.R.Brooks,and J.J.V.Kasper J.Chem.Phys. 55, 1980 (1971)

23) F.Heismann and H.J.Loesch Chem.Phys. 64, 43 (1982)
M.Hoffmeister, L.Potthast, and H.J.Loesch Chem.Phys. 78, 369 (1983);
M.Hoffmeister, R.Schleysing, and H.J.Loesch J.Phys.Chem. 91, 5441 (1987);
M.Hoffmeister, R.Schleysing, F.Stienkemeyer, and H.J.Loesch J.Chem.Phys. 89, 3528 (1989)

24) A.Gupta, D.S.Perry, and R.N.Zare J.Chem.Phys.72, 6250 (1980);
D.J.Rakestraw, K.G.McKendrick, and R.N.Zare J.Chem.Phys. 87, 7341 (1987);
R.Zhang, D.J.Rakestraw, K.G.McKendrick, and R.N.Zare Chem.Phys. 89, 6283 (1988)

25) C.V. Boughton, R.E. Miller, and R.O. Watts Austral. J. Phys. 35, 611 (1982)
P.F. Vohralik, R.E. Miller, and R.O. Watts J. Chem. Phys. 93, 2182 (1989)

26) L.J. Pawluk and M. Keil J. Opt. Soc. Am. B6, 1278 (1989)

27) S.H.Kable and A.E.W.Knight J.Chem.Phys. 86, 4709 (1987);
A.B.Rock, C.M. Van Zoeren, S.H.Kable, G.B.Edwards, and A.E.W.Knight J.Chem.Phys. 89, 6777 (1988);
E.Carrasquillo, A.L.Utz and F.F.Crim J.Chem.Phys. 88, 5976 (1988)

28) M. Broyer, G. Delacretaz, G.Q. Ni, R.L. Whetten, J.P. Wolf and L. Wöste, J. Chem. Phys. 90, 4620, (1989)
Y.S. Choi and C.B. Moore J. Chem. Phys. 90, 3875 (1989)
E.A. Rohlfing and J.E.M. Goldsmith J. Chem. Phys. 90, 6804 (1989)

29) A.Geers, J.Kappert, F.Temps, and J.W.Wiebrecht Chem.Phys.Lett 155 614 (1989)

30) X.Yang and A.M.Wodtke J.Chem.Phys. in print

31) N.Bloembergen Am.J.Phys. 35, 989 (1967)

32) J.C.White in "Topics in Applied Physics: Tunable Lasers, L.F.Mollenhauer and J.C.White, Springer Verlag, New York (1987)

33) A.P. Peirce, M.A. Dahleh, and H. Rabitz Phys.Rev.A 37, 4950 (1988)
S. Shi, A. Woody, and H. Rabitz, J. Chem. Phys. 88, 6870 (1989)

34) P.R.Berman and R.Salomaa Phys.Rev. A 25, 2667 (1982)

35) W.S.Warren and A.H.Zewail J.Chem.Phys. 78, 3583 (1983)

36) W.S.Warren and M.Haner in: Atomic and molecular processes with short intense laser pulses", A.D.Bandrauk ed., NATO ASI Series B, Vol 171, Plenum Press, New York (1988)

37) W.S.Warren J.Chem.Phys.81, 5437 (1984)

38) W.S.Warren, J.L.Bates, M.A.McCoy, M.Navratil, and L.Mueller J.Opt.Soc.Am. B 3, 488 (1986);
M.R. Banash and W.S. Warren, Laser Chem. 6, 47 (1986)

39) J.Oreg, F.T.Hioe, and J.H.Eberly Phys.Rev. A 29, 690 (1984)

40) J.Oreg, G.Hazak, and J.H.Eberly Phys.Rev. A, 2776 (1985)

41) F.T.Hioe and J.H.Eberly Phys.Rev.Lett 47, 838 (1981)

42) F.T.Hioe and J.H.Eberly Phys.Rev. A 25, 2168 (1982)

43) F.T.Hioe Phys.Rev. A 28, 879 (1983); F.T.Hioe Phys.Lett 99A, 150 (1983)

44) J.R.Kuklinski, U.Gaubatz, F.T.Hioe, and K.Bergmann Phys.Rev A to be published

45) C.E.Carroll and F.T.Hioe J.Phys.A: Math.Gen 19, 2061 (1986);
C.E.Carroll and F.T.Hioe Phys.Rev. A, 724 (1987)
F.T.Hioe and C.E.Carroll Phys.Rev A 37, 3000 (1988)
C.E.Carroll and F.T.Hioe J.Math.Phys. 29, 487 (1988)

46) C.E.Carroll and F.T.Hioe J.Opt.Soc.Am B 5, 1335 (1988)
F.T.Hioe J.Opt.Soc.Am. B 4, 1327 (1987);

47) C.E.Carroll Phys.Rev.A 39, 2243 (1989)
C.E. Carroll and F.T. Hioe J. Phys. B: At. Mol. Opt. Phys 22, 2633 (1989)

48) G.L.Peterson, C.D.Cantrell, and R.S.Burkey Opt.Commun. 43, 123 (1982)

49) U.Gaubatz, P.Rudecki, M.Becker, S.Schiemann, M.Külz, and K.Bergmann Chem.Phys.Lett. 149, 463 (1988)

50) C.Liedenbaum, S.Stolte, and J.Reuss Phys.Rep, 178, 1 (1989)

51) R.L.Shoemaker in: "Laser and Coherent Spectroscopy" J.I.Steinfeld ed, Plenum Press, New York (1984)

52) L.Allen and J.H.Eberly "Optical Resonance and Two-Level Atoms", John Wiley and Sons, New York (1974)

53) S.Stenholm "Foundation of Laser Spectroscopy" John Wiley and Sons, New York (1984)

54) S.M.Hamadani, A.T.Mattick, N.A.Kurnit, and A.Javan Appl.Phys.Lett 27, 21 (1975);
S.Avrillier, J.M.Raimond, Ch.J.Bordé, D.Bassi, G.Scoles Opt.Commun. 39, 311 (1981);
A.G.Adams, T.E.Gough, N.R.Isenor, and G.Scoles Phys.Rev.A 32, 1451 (1985);

55) J.P.C.Kroon, H.A.J.Senhorst, H.C.W.Beijerinck, B.J.Verhaar, and N.F.Verster, Phys.Rev.A 31, 3724 (1985)

56) R.G.Hulet and D.Kleppner Phys.Rev.Lett 51, 1430 (1983);
W.A.Molander, C.R.Strout, and J.A.Yeazell J.Phys.B: At.Mol.Phys. 19, L461 (1986)

57) M.M.T.Loy Phys.Rev.Lett. 32, 814 (1974);
M.M.T.Loy Phys.Rev.Lett. 41, 473 (1978)

58) Grischkowsky and M.M.T.Loy Phys.Rev.A 12, 1117 (1975);
D.Grischkowsky, M.M.T.Loy, and P.F.Liao Phys.Rev.A 12, 2514 (1975);
M.D.Crisp Phys.Rev.A 8, 2128 (1973)

59) A.E.de Priisto, H. Rabitz, and R. Miles J.Chem.Phys. 73, 4798 (1980)
F.Shimizu, K.Shimizu, and H.Takuma Chem.Phys.Lett 102, 375 (1983);
F.Shimizu, K.Shimizu, and H.Takuma Phys.Rev. a 31, 3132 (1985)

60) M.Becker, U.Gaubatz, P.L.Jones, and K.Bergmann J.Chem.Phys.87, 5064 (1987)

61) C.Cohen-Tannoudji in "Frontiers in Laser Spectroscopy I", B.Balian, S.Haroche, S.Liberman, eds. , North Holland, (1977)
C.Cohen-Tannoudji and S.Reynaud J.Phys.B: At.Mol.Phys. 10, 345 and 365 (1977);
C.Cohen-Tannoudji and S.Reynaud in "Multiphoton Processes" J.H.Eberly and P.Lambropoulos eds., John Wiley and Sons, New York (1978);
J.Dalibard and C.Cohen-Tannoudji J.Opt.Soc.Am. B 2, 1707 (1985)

62) C.Cohen-Tannoudji and S.Reynaud J.Phys.B: At.Mol.Phys. 10, 2311 (1977)

63) G.Alzetti, A.Gozzini, L.Moi, and G.Orriols Nuovo Cimento B36, 5 (1976);
E.Arimondo and G.Orriols Lett. Nuovo Cimento 17, 333 (1976)
E. Arimondo in "Interaction of Radiation and Matter, eds. G. Alezetto, E. Arimondo, F. Bassani, and L. Radicati Scuola Normale Superiore, Quaderni (Pisa), (1987)

64) H.R.Gray, R.M.Whitley, and C.R.Stroud,Jr. Opt.Lett. 3, 218 (1978);

65) M.Kaivola, N.Bjerre, O.Poulson, and J.Javanainen Opt.Commun. 49, 418 (1984);

66) F.R.McLean, R.J.Ballagh, and D.M.Warrington J.Phys.B: At.Mol.Phys 18, 2371 (1985)

67) S.Swain J.Phys.B: At.Mol.Phys. 15, 3405 (1982)

68) A.Aspect, E.Arimondo, R.Kaiser, N.Vansteenkiste, and C.Cohen-Tannoudji Phys.Rev.Lett 61, 826 (1988)

69) K.K.Verma, T.Vu, and W.C.Stwalley J.Mol.Spectr. 85, 131 and 150 (1981);
K.K.Verma, J.T.Bahns, A.R.Rajaei, W.C.Stwalley, and W.T.Zemke J.Chem.Phys. 78, 3599 (1983)

70) G.Herzberg "Molecular Spectra and Molecular Structure, Spectra of Diatomic Molecules", Von Nostrand Reinhold Comp., New York (1950)

71) P.L.Knight and P.W.Miloni Phys.Rep. 66, 21 (1980)

72) S.Stenholm and R.Salomaa in Proc.of the Conf. on Lasers in Chemistry, London 1977, p.251

73) W.Demtröder "Laser Spectroscopy", Springer Series in Chemical Physics, Springer Verlag, Berlin (1981), p.100

74) W.Demtröder, W.Stetzenbach, M.Stock, and J.Witt J.Mol.Spectr. 61, 382 (1976);

75) G.Gerber and R.Moeller Chem.Phys.Lett 113, 546 (1985)

76) M.D.Levenson and S.S. Kano "Introduction to nonlinear Laser spectroscopy, Academic Press, New York, 1988

77) see Chapter 9 of ref 3

78) K.Bergmann and E.Gottwald Chem.Phys.Lett. 78, 515 (1981)

79) M.Becker PhD Thesis, Universität Kaiserslautern 1987

80) K.Bergmann, U.Hefter, and P.Hering Chem.Phys. 32, 329 (1978);
K.Bergmann, R.Engelhardt, U.Hefter, and P.Hering Chem.Phys. 44, 23 (1979)

81) F.Aerts, H.Hülsman, and P.Willems Chem.Phys. 68, 233 (1982)

82) A.Yariv, "Quantum Electronics" John Wiley and Sons, New York (1975)

83) K.Bergmann, R.Engelhardt, U.Hefter, and J.Witt J.Phys.E: Sci Instrum. 12, 507 (1979);
see also ref. 3, Chapter 9

84) I. Littler, P. Jung, and K. Bergmann, to be published
P.Jung Diplom thesis, Universität Kaiserslautern (1989)

85) see ref 3, Chapter 9, Fig. 9.30

86) Y.S.Bai, A.G.Yodh, and T.W.Mossberg Chem.Phys.Lett. 55, 1266 1985)

87) A.E. Siegman "Lasers" Uni. Science Books (1986)

88) A.Messiah, Quantum Mechanics, Vol.II, North-Holland, Amsterdam (1962), p.744

89) C.P. Slichter "Principles of Magnetic Resonance" Springer Verlag Berlin (1988)

90) T.S. Ho and S.I. Chu Phys. Rev. A 31, 659 (1985)

91) A.C. Albrecht J. Chem. Phys. 34, 1476 (1961)

92) U. Gaubatz, S. Schiemann, A. Kuhn, and K. Bergmann
to be published

Table I Spectroscopic data for the Na_2 (A - X) transition relevant for this experiment. The lifetime of the A-state is τ_{sp} = 12.5 ns corresponding to an electronic transition dipol moment $\mu_{el} \approx 10$ debye[a]. The line strength factor for the R-transition used here is L = 0.55.

transition	(v",j")-(v',j')	wavelength (nm)	FCF[b]
1 -- 2[c]	(0,5) - (7,6)	646.790	0.113
3 -- 2[d]	(5,5) - (7,6)	680.852	0.051
3 -- 5[e]	(5,5) - (12,6)	656.240	0.038

a) ref [69]; b) ref.[74, 75]; c) pump laser transition;
d) Stokes laser transition; e) probe laser transition.

Table II Rabi-frequencies in units of 10^9 s^{-1} for transitions specified in Table I

Intensity transition	10^{-2} mW/mm^2	1 mW/mm^2	10^2 mW/mm^2
1 -- 2	0.013	0.129	1.29
3 -- 2	0.009	0.087	0.87

Table III Efficiency and width of $E(\Delta_s)$ for various detunings Δ_p and Rabi frequencies $\Omega_p = \Omega_s = 0.7\ 10^9\ s^{-1}$

$\Delta_p/2\pi$ [MHz]	$E(\Delta_s=0)$ [a]	width of $E(\Delta_s)$ [b] [MHz]
0	> 75%	35
500	≈ 20%	20
840	≈ 15%	15
1120	≈ 10%	10

a) These data are likely to be improved with better frequency stability of the lasers.

b) Full width at half maximum. The uncertainty is about ± 3 MHz.

Figure Captions

Fig.1: Representative 3-level system with levels 1,2 and 3, coupled by the pump and Stokes laser. The relevant Rabi frequencies $\Omega_{p,s}$ and detuning $\Delta_{p,s}$ of the laser frequencies from the transition frequencies as well as the spontaneous decay rates A_{2k} of level 2 are indicated. Two-photon (Raman-) resonance requires $\Delta_p = \Delta_s$. Level 4 summarizes all other levels accessible by dipole radiation from level 2. Under our experimental conditions, the rate k_{41} for collisional coupling between levels 4 and 1, is zero. The rate k_{2n} of removal of population from level 2 by processes such as ionization or predissociation (see dashed arrow) is also assumed to be zero. The population of level 3 is probed, at a different location, by laser induced fluorescence via level 5.

Fig.2: Schematic experimental set-up with the molecular beam and the pump-, Stokes- and probe laser beams, delivered to the apparatus from the lasers by single mode polarization preserving optical fibres. Distances as well as the diameter of collimating apertures are given in mm. The main and auxiliary detectors D1 and D2, respectively, as also shown.

Fig.3: Typical raw data with the pump laser frequency tuned to near resonance with the transition from level 1 to 2, (a) and (b), or 240 MHz off resonance (c) as the Stokes laser frequency is tuned across the resonance (see Table I and Fig. 1). The axes of the pump- and Stokes laser coincide for the data shown in (a) but are suitably displaced for those shown in (b) and (c). The dashed line gives the intensity level related to the population of level 3 by spontaneous emission only.

Fig.4: The efficiency of population transfer from level 1 to level 3 for $\Delta_p = \Delta_s = 0$ as the spatial separation D of the laser beam axes is varied. D is measured in units of the beam waist w_L. Negative values of D correspond to a configuration with

the Stokes laser preceeding the pump laser, see upper panel of the figure. When considering propagation times of molecules through the beams we have, see eq. (14), $\eta = -0.5$ for $D/w_L = -1$.

Fig.5: Same as Fig.4 but with both lasers tuned 400 MHz off resonance.

Fig.6: Variation of the transfer efficiency in the case of optimum displacement of the laser beam axes as the Stokes laser frequency is tuned across the resonance. The base line is slightly asymmetric because the pump laser detuning Δ_p is not exactly zero (see also Fig. 3).

Fig.7: Observation of the correlation between the population transfer efficiency and the decrease in the fluorescence from the interaction region of the pump and Stokes laser with the molecular beam, observed with detector D2, see Fig. 2.

Fig.8: From top of the bottom, the variation of the Rabi frequencies $\Omega_{p,s}$ and of the eigenvalues ω^0 and $\omega^\pm$ for $\Delta_p > 0$, $\Delta_p = 0$ and $\Delta_p < 0$, see eq.(6), is shown as a function of the reduced time $\tau = t/\Delta\tau$.

Fig.9: Evolution of the population in levels 1, 2 and 3, given by the corresponding density matrix elements for optimum displacement of the laser beam axes (left panels), coinciding axes (middle panels) and reverse ordering (pump laser preceeding Stokes laser, right panels). The spatial separation D and the delay in terms of the propagation time are related by eq. (14), with $|\eta| = 0.6$ corresponding to $|D| = 1.2\ w_L$. The insert shows an enlarged portion of the main figure, using the same scale τ. The vertical scale runs from 0 to 0.03. The "reverse" STIRAP process (population transfer from level 3 back to level 1) is clearly seen.

Fig.10: Summary of the flow of population from the initially populated level 1 ($n_0 \simeq 100$) via the states $|a^0\rangle$ and $|a^\pm\rangle$ to the levels 1 and 3 for characteristic geometric arrangments ($D < 0$, $D = 0$ and $D > 0$) as well as characteristic detuning ($\Delta > 0$, $\Delta = 0$ and $\Delta < 0$ with $\Delta_p = \Delta_s = \Delta$). The asymptotic value of the relevant mixing angles is also given. The diagrams are explained in the upper left panel. The step in the lines connecting state $|1\rangle$ with $|a^\pm\rangle$ indicates which one of the level $|a^\pm\rangle$ is non degenerate with the others for $\Omega_{p,s} = 0$, see Fig. 8. The width of the arrows leading out of the states $|a^\pm\rangle$ correlates qualitatively with the radiative damping of these states. The arrows leading out of level 3 for $D > 0$ relate to the optical depletion process discussed in Sect V B4 and seen at the right hand side of Fig. 9.

Fig.11: Variation of the calculated maximum transfer efficiency E_{max} and the quantity $\Omega_0\Delta\tau$ (see eq.(18), $F^* = 5$) for $\Omega_0 = 10^9\ s^{-1}$ and $\Delta_{p,s} = 0$ as the overlap $\eta = \frac{D}{2u\Delta\tau}$ (see eq. (14)) of the laser beams is varied. The function F/F^* is discussed in Sect. VD. Adiabatic following around $\tau = 0$ is maintained as long as $F/F^* < 1$.

Fig.12: Comparison of the STIRAP process in a three level system (d) with the π-pulse technique (a) and rapid adiabatic passage method (b) in a two - level system in the Bloch-vector picture. The variation of the first and third component of the vector F (see eq.(22)) for the STIRAP process is shown in part (c).

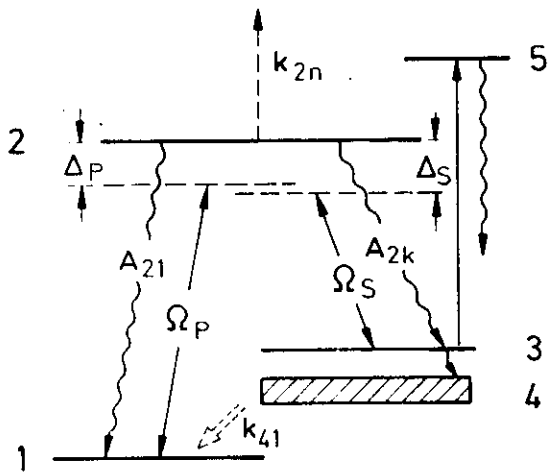
k_{2n}
5
2
Δ_P
Δ_S
A_{21}
A_{2k}
Ω_S
Ω_P
3
4
k_{41}
1

Fig 1

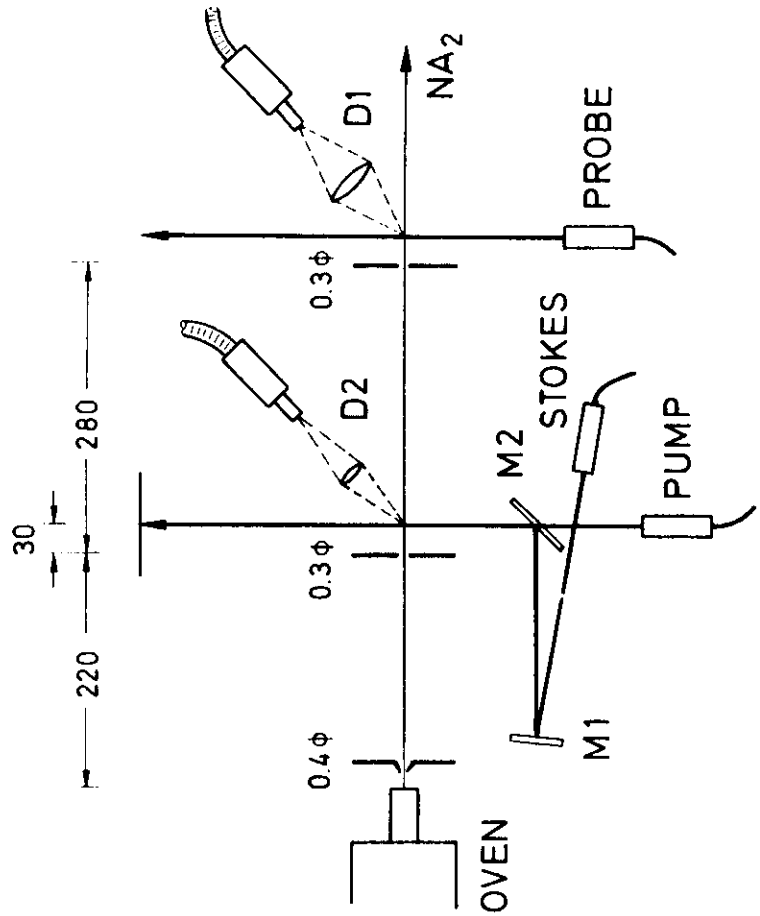
D1
NA_2
PROBE
0.3Φ
D2
STOKES
M2
PUMP
280
30
220
0.3Φ
0.4Φ
M1
OVEN

Fig 2

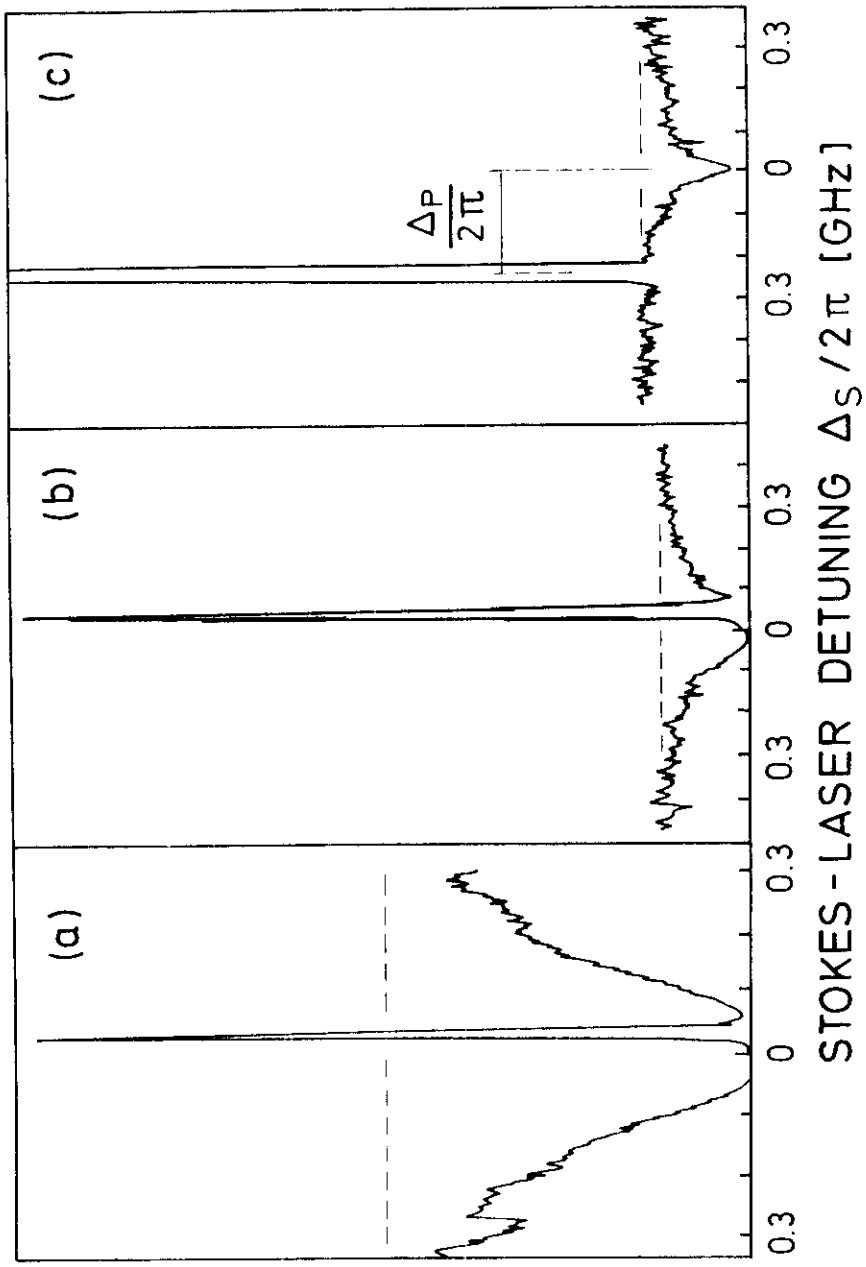
(c)
(b)
(a)
$\frac{\Delta_P}{2\pi}$
0.3
0
0.3
0.3
0
0.3
0.3
0
0.3
STOKES-LASER DETUNING $\Delta_S/2\pi$ [GHz]

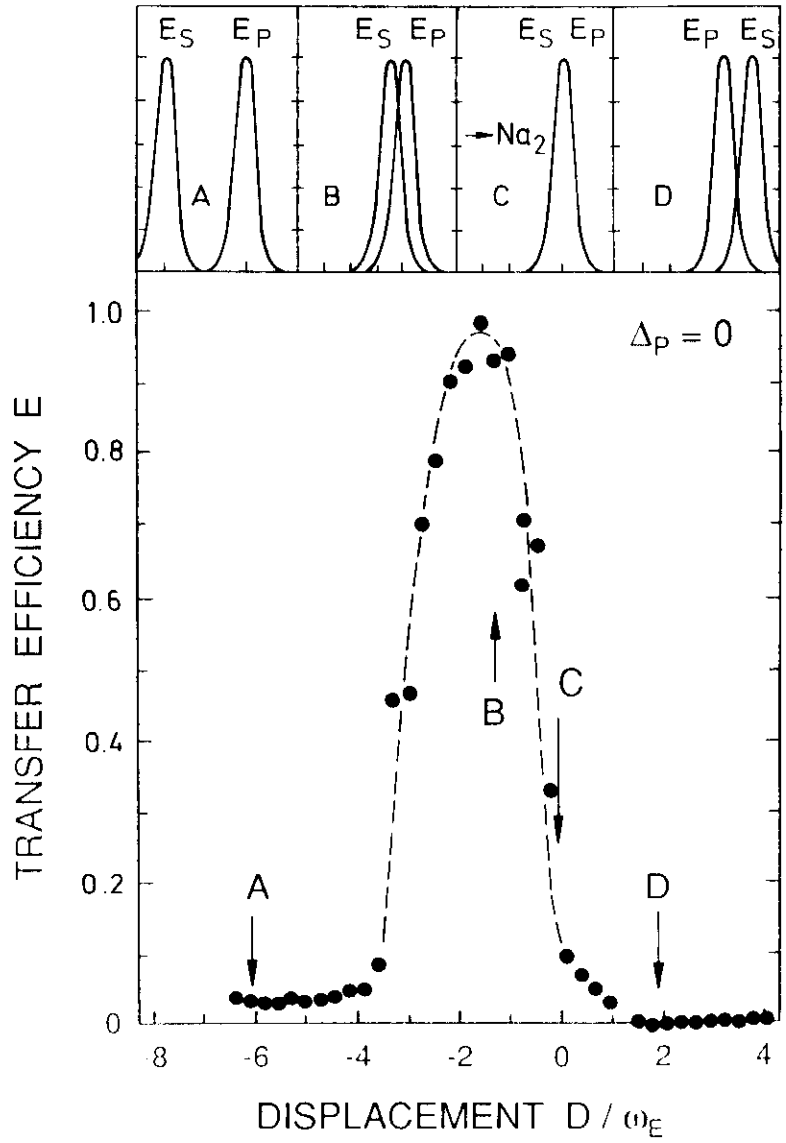
E_S E_P
A
E_S E_P
B
E_S E_P
Na_2
C
E_P E_S
D
$\Delta_P = 0$
TRANSFER EFFICIENCY E
1.0
0.8
0.6
0.4
0.2
0
A
B
C
D
8
-6
-4
-2
0
2
4
DISPLACEMENT D/ω_E

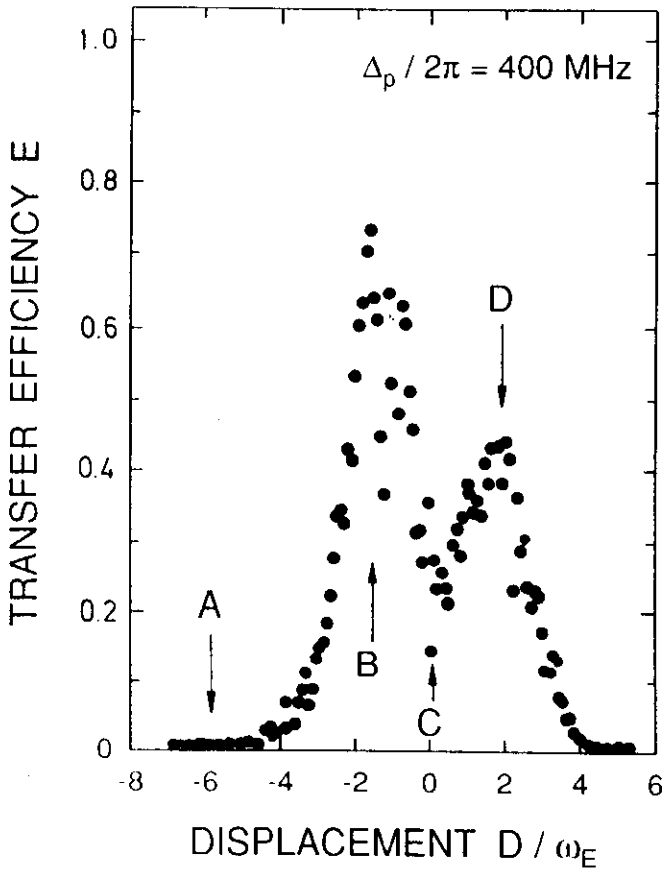
TRANSFER EFFICIENCY E
1.0
0.8
0.6
0.4
0.2
0
$\Delta_p / 2\pi$ = 400 MHz
A
B
C
D
-8
-6
-4
-2
0
2
4
6
DISPLACEMENT D / ω_E

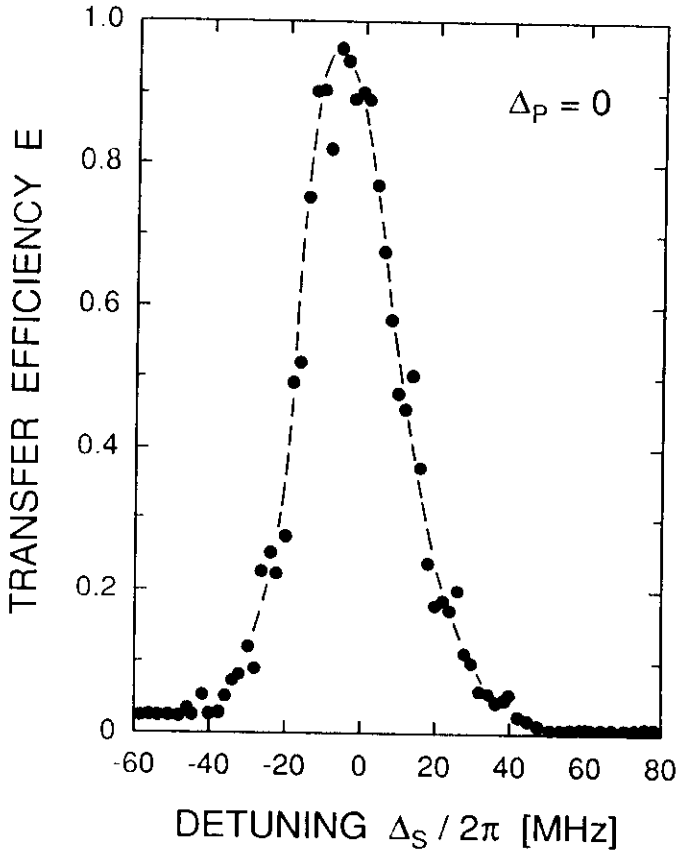
TRANSFER EFFICIENCY E
1.0
0.8
0.6
0.4
0.2
0
Δ_P = 0
-60
-40
-20
0
20
40
60
80
DETUNING $\Delta_S / 2\pi$ [MHz]

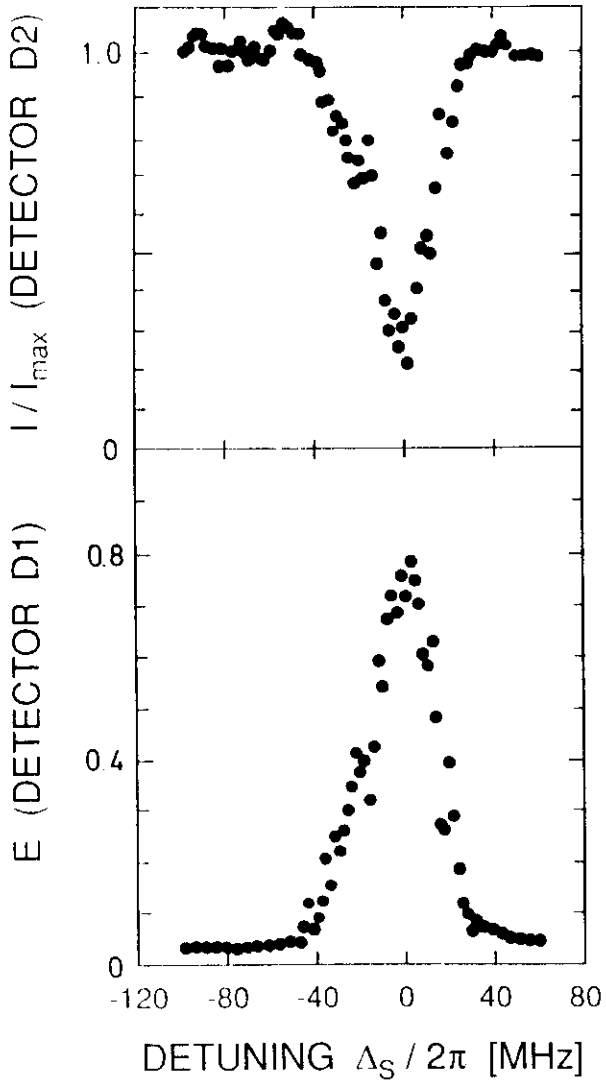
E (DETECTOR D1)
I / I_max (DETECTOR D2)
1.0
0
0.8
0.4
0
-120
-80
-40
0
40
80
DETUNING Δ_S / 2π [MHz]

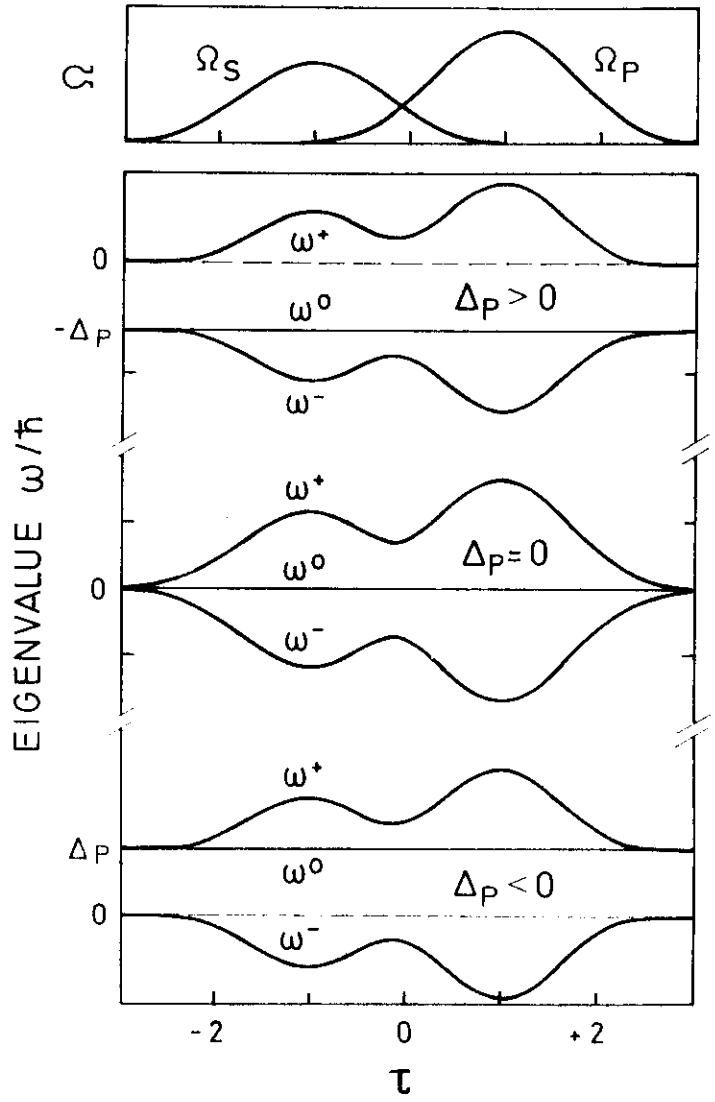
Ω
Ω_S
Ω_P
EIGENVALUE ω/ħ
ω+
ω°
ω⁻
0
-Δ_P
Δ_P > 0
Δ_P = 0
Δ_P
Δ_P < 0
-2
0
+2
τ

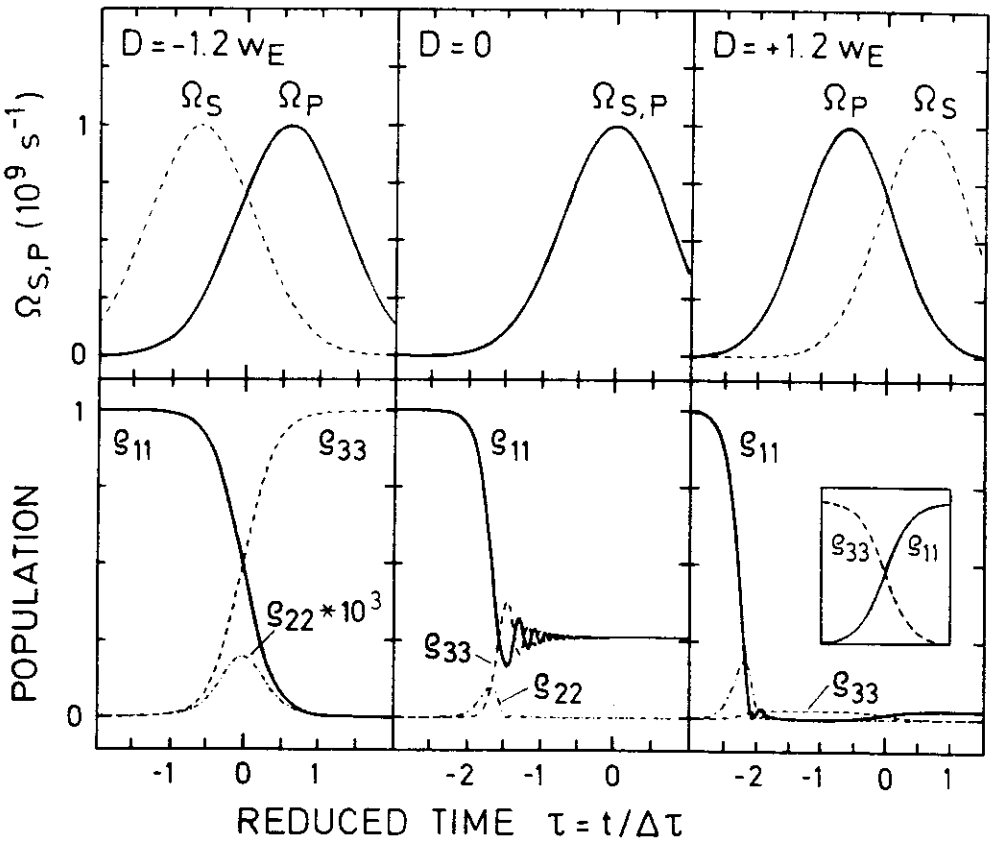

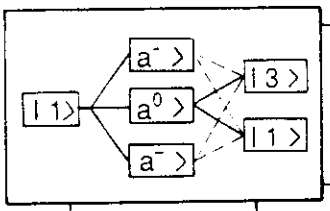

	D < 0 cos Θ(-∞) = 1 sin Θ(+∞) = 1	D = 0 cos Θ = $2^{-1/2}$ sin Θ = $2^{-1/2}$	D > 0 cos Θ(-∞) = 0 sin Θ(+∞) = 0
Δ > 0 cos ϕ = 0 sin ϕ = 1	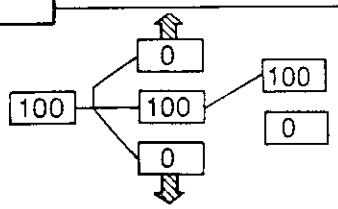	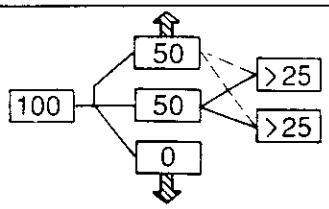	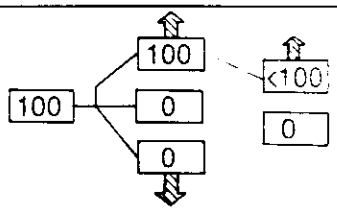
Δ = 0 cos ϕ = $2^{-1/2}$ sin ϕ = $2^{-1/2}$	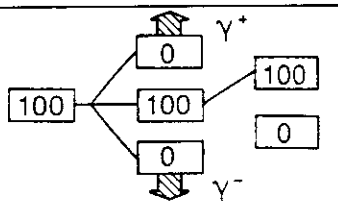	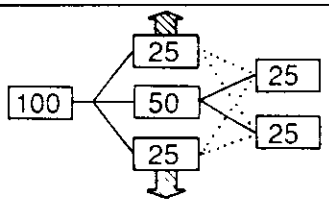	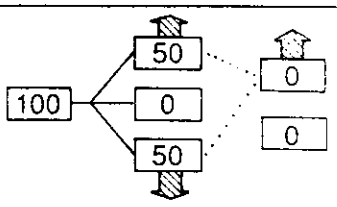
Δ < 0 cos ϕ = 1 sin ϕ = 0	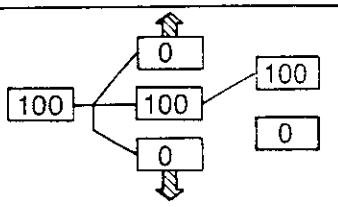	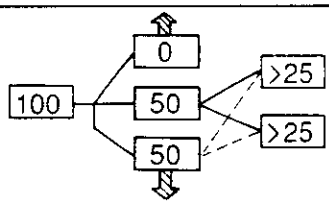	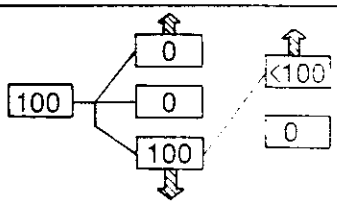

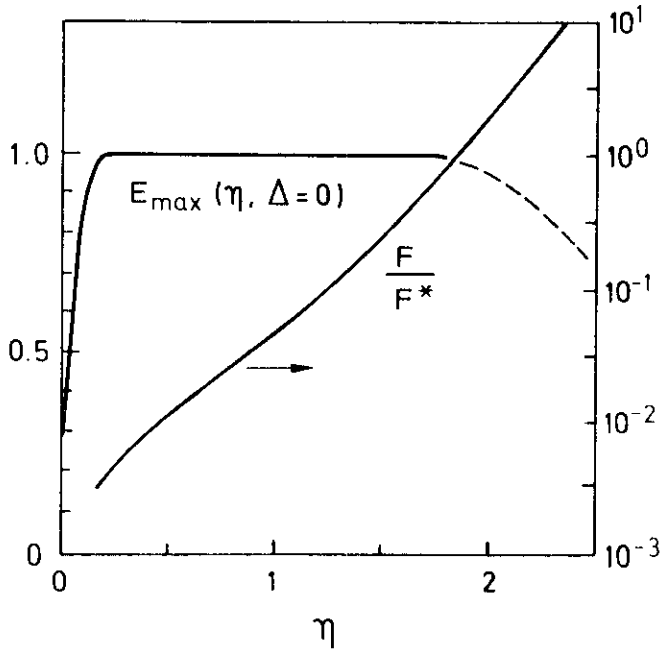
1.0
0.5
0
0
1
2
η
E_{max} (η, Δ = 0)
F / F*
10^{1}
10^{0}
10^{-1}
10^{-2}
10^{-3}

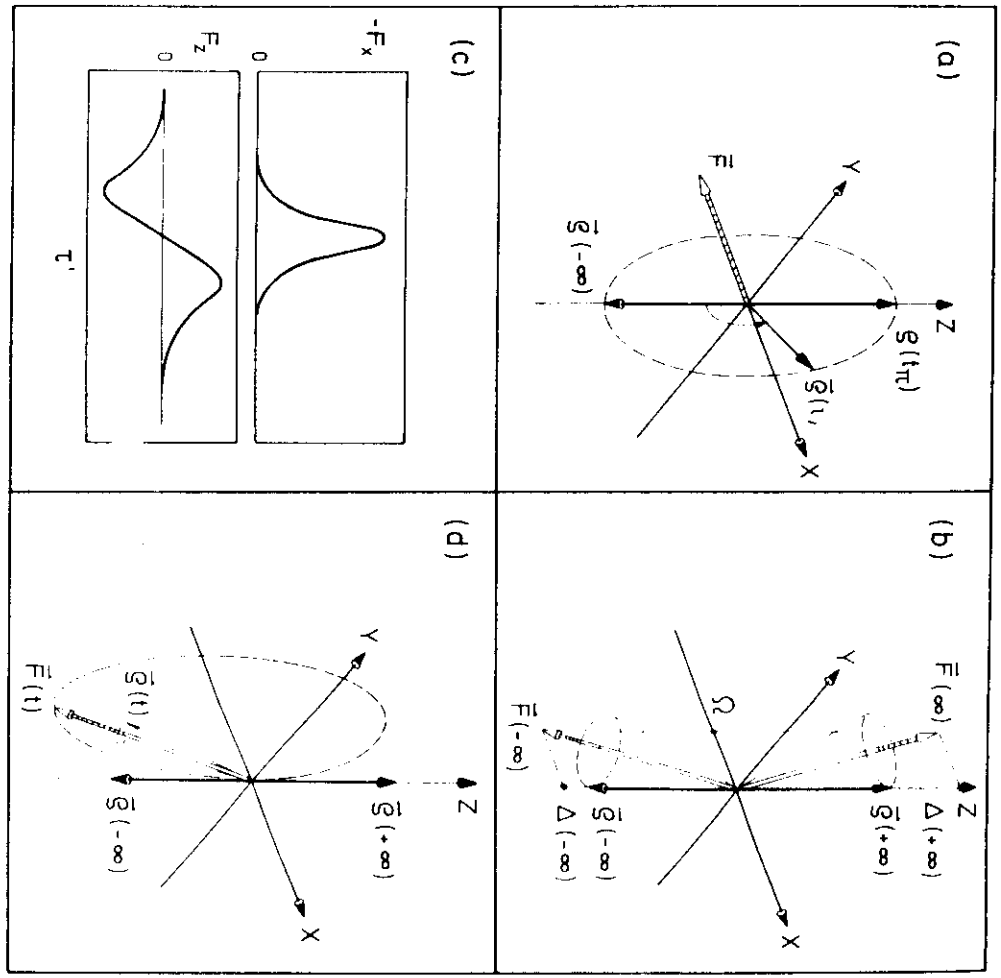
(a)
(b)
(c)
(d)
F
Y
Z
X
$\vec{\varrho}(-\infty)$
$\vec{\varrho}(t_\pi)$
$\vec{\varrho}(t_f)$
F_z
$-F_x$
0
τ
Ω
$\vec{F}(\infty)$
$\vec{F}(-\infty)$
$\vec{\Delta}(+\infty)$
$\vec{\Delta}(-\infty)$
$\vec{\varrho}(+\infty)$
$\vec{F}(t)$
$\vec{\varrho}(t)$